This dissertation has been
microfilmed exactly as received

68-13,331

HO, Norman F. H., 1931-

INTERACTION OF PARTICULATE MATTER IN LIQUID SYSTEMS OF BIOPHARMACEUTICAL IMPORTANCE.

The University of Michigan, Ph.D., 1968
Health Sciences, pharmacy

University Microfilms, Inc., Ann Arbor, Michigan

INTERACTION OF PARTICULATE MATTER IN LIQUID SYSTEMS OF BIOPHARMACEUTICAL IMPORTANCE

By
Norman F. H. Ho

A dissertation submitted in partial fulfillment
of the requirements for the degree of
Doctor of Philosophy in the
University of Michigan
1968

Doctoral Committee:

Professor William I. Higuchi, Chairman
Associate Professor Joseph P. Chandler
Assistant Professor Donald L. Rucknagel
Assistant Professor Anthony P. Simonelli
Associate Professor George Zografi

INTERACTION OF PARTICULATE MATTER IN LIQUID SYSTEMS OF BIOPHARMACEUTICAL IMPORTANCE

By Norman F. H. Ho

Abstract

Methods for the quantitative mechanistic study of certain areas in the formation, growth, flocculation or coalescence behavior of particles in liquid systems of great importance in biopharmaceutics, clinical biochemistry and biology were developed. Theoretical considerations of flocculation kinetics and particle-particle interactions were reviewed and, in some instances, were further extended.

A theoretical study of preferential coalescence and aggregation of small particles in heterodispersed systems has been carried out where moderate electrical barriers exist between the particles. Equations based on the concepts of Derjaguin, Verwey, and Overbeek were employed. Computations over a wide range of conditions have shown that small particles may aggregate (or coalesce) with themselves or with larger particles at rates that are ten to fifty orders of magnitude faster than particles ten times larger. These findings may explain (a) the relatively narrow particle size distributions observed in certain emulsions and flocculated suspensions and (b) the limited flocculation and coalescence behavior observed in certain instances.

A method of studying the kinetics and mechanisms of flocculation of denatured protein particles was developed. It was found that a procedure based on the RIDL multichannel particle counter and size analyzer system was suitable. The precipitation behavior of urea denatured ovalbumin was studied near its isoelectric point. An evaluation of the data showed that the Smoluchowski theory for rapid flocculation of monodispersed particles and the self-preservation theory satisfactorily accounted for the results.

Particle size distributions found in parenteral solutions were determined using the Coulter counter. Its significance pertaining to potential clinical reactions and standards of clarity of parenteral products is discussed.

TO

Mary and Children,

Mother and Father

ACKNOWLEDGEMENTS

It is not at all easy to give adequate recognition to all those individuals who have contributed in some way towards the accomplishments of my research. To all of them I wish to express my sincere gratitude. However, there are certain persons whom I want to acknowledge especially.

To Dr. William I. Higuchi, I am indebted to his expert guidance and keen interest in this study and my academic goals. His constant involvement in research, often at the expense of personal consideration and time, represents a labor of love and dedication to research on a high level basis.

I wish to acknowledge Dr. Donald E. Francke for his friendship and general advice.

To the members of my Doctoral Committee, I owe many thanks for their suggestions in the preparation of this thesis.

To Miss Sandra McCullough and Mr. William Mies, I am grateful for their assistance in the preparation of this manuscript.

Finally, I wish to acknowledge the support of the Institute of General Medical Sciences, National Institutes of Health, U.S. Public Health Service under fellowship 5 - F1 - GM - 24,039.

TABLE OF CONTENTS

ACKNOWLEDGEMENTS iii

LIST OF TABLES vi

LIST OF FIGURES vii

INTRODUCTION 1

LITERATURE REVIEW 3

- Preferential Flocculation and Coalescence in Heterodispersed Systems 3
- Flocculation and Sedimentation Behavior in Biochemical Systems 5
- Macroaggregates of Denatured Proteins 8
- Particulate Matter in Parenteral Solutions 8

STATEMENT OF THE PROBLEM 11

SECTION I: THEORIES OF FLOCCULATION 13

- Smoluchowski Theory of Rapid Flocculation of Monodispersed Systems 13
- Rapid Flocculation of Heterodispersed Systems 14
- General Particle Size Distribution Effects on the Rate of Flocculation 16
- Similarity or Self-Preserving Theory 20
- Slow Flocculation 22

SECTION II: PREFERENTIAL FLOCCULATION AND COALESCENCE OF HETERODISPERSED SYSTEMS 24

- Theory 24
- Calculations 28
- Discussion 28

SECTION III: KINETICS OF FLOCCULATION OF DENATURED PROTEINS 44

Experimental 45

Results and Discussion 61

SECTION IV: QUANTITATIVE STUDIES OF PARTICULATE MATTER IN PARENTERAL SOLUTIONS 74

Experimental 74

Results and Discussion 77

SUMMARY AND CONCLUSIONS 84

APPENDICES

I. Attractive Potential Energy between Unequal Spheres and the Effect of Retardation 86

II. Repulsive Potential Energy between Unequal Spheres 92

III. Interaction Potential Energies between a Sphere and an Infinitely Large Flat Plate 93

LIST OF REFERENCES 99

LIST OF TABLES

Table		Page
I	Relationship between the Debye-Huckel K and the Electrolyte Concentration	30
II	Summary of Data on the Influence of Electrolyte Concentration (K), Surface Potential (ψ_o) and the Hamaker Constant (A) on the Maximum Potential Interaction Energy of the Barrier (V_{Tmax}) and the Rate Constant for Flocculation (G')	36
III	Comparison of Coulter Counter, Model A, and the RIDL Multichannel Data on Mixed Latex Particles	60
IV	Summary of Data on the Flocculation of Urea-Denatured Ovalbumin	68
V	Comparison of Methods of Determining Rate Constants of Flocculation	72
VI	Possible Cumulative Number of Particles in a Typical Intravenous Solution Prescription	83

LIST OF FIGURES

Figures		Page
1.	Geometrical Consideration of Two Interacting Spheres of Equal Radii.	15
2.	Probability of Rapid Flocculation between Particles of Different Sizes when the Stability Factor W_{ij} Equals Unity.	17
3.	Influence of Particle Sizes on the Total Potential Energy of Interaction. A = 5×10^{-13} ergs, ψ_o = 25 mv and K = 2×10^6 cm^{-1}.	31
4.	Influence of Electrolyte Concentrations on the Total Potential Energy of Interaction for Two Particle Sizes. A = 1×10^{-13} ergs and ψ_o = 25 mv.	32
5.	Influence of Surface Potential on the Total Energy of Interaction for Two Particle Sizes. A = 5×10^{-13} ergs and K = 2×10^6 cm^{-1}.	34
6.	Rate Constant (G') as a Function of Concentration of 1-1 Electrolyte for Various Particle Sizes. A = 1×10^{-13} ergs and ψ_o = 25 mv.	38
7.	Rate Constant (G') as a Function of Concentration of 1-1 Electrolyte for Various Particle Sizes. A = 5×10^{-13} ergs and ψ_o = 25 mv.	40
8.	RIDL Multichannel Particle Counter and Size Analyzer System.	48
9.	Differential Distribution Data for a Mixture of 1.17 and 1.72-μ Diameter Latices. Two-Hundred Channels Used.	50
10.	Same Distribution as Fig. 9, But Only the First One-Hundred Channels Presented.	53
11.	Analysis of a Mixture of 1.17-μ and Aggregated 1.72-μ Diameter Latices.	54

Figures Page

12. Distribution Curves Accounting for Additivity in a Polydispersed Latex System by the RIDL Multichannel Analyzer. 58

13. Differential Distribution Data Showing Flocculation of Denatured Ovalbumin Particles with Time in Buffered Saline, pH = 4.6. 63

14. Changes in Total Denatured Protein Particulate Concentration for Sizes Greater Than 0.80-μ Diameter as a Function of Time. 64

15. Linear Plots Showing Agreement of the Flocculation-Time Data with the Smoluchowski Theory. 67

16. Cumulative Size Distributions for Flocculating Denatured Ovalbumin Particles. 70

17. Test of Self-Preservation Theory for Flocculating Denatured Ovalbumin Particles. 71

18. Sampling Chamber for the Coulter Counter Used for the Determination of Particle Size Distributions in Parenteral Solutions. 76

19. Cumulative Particle Size Distributions in Normal Saline for Injection in One Liter Containers. 78

20. Cumulative Particle Size Distributions in Vials Containing Penicillin G Potassium and Chloramphenicol Sodium Succinate. 80

21. Geometry of the London-Van der Waal Interaction between an Atom and an Infinitely Large Flat Plate. 88

22. Illustrating the Building Up of Attraction between Two Unequal Spheres via Parallel Flat Plates. 90

23. Geometry of the London-Van der Waal Interaction between a Sphere and an Infinitely Large Flat Plate. 95

24. Geometry of Interacting Quasi-Parallel Electrical Double Layers between a Sphere and an Infinitely Large Flat Plate. 97

INTRODUCTION

Our understanding of the formation, growth, aggregation or coalescence behavior of particles in liquid systems is of great importance in biopharmaceutics and other areas of biology. In certain aspects of biopharmaceutics one is concerned with the physical nature of the dosage form and the processes by which the dosage form is manufactured as they are related to the nature and intensity of the biological effects. The surface and flow properties help to characterize the dispersed particles, and to a great extent the formulation of special products is concerned with these properties alone. One measure of the stability of these products is the degree of dispersion with time or, when the dispersion is in the flocculated and sedimented state, the ease of redispersion. Provided that the biological absorption is rate-limited by the dissolution process of solid particles or by the simple diffusion of drug from emulsion droplets, a large, effective surface area in contact with the interacting liquid medium would result in rapid absorption rates.

The biologically important colloids, e.g., the proteins, are fine particles upon which the life processes depend. For this reason, many diseases are diagnosed on

the basis of abnormal concentrations of certain proteins and blood cells and their physico-chemical behavior in in vitro tests. Particles may even subject the life process to threats of illness and death, for example, by anaphylactic reactions to foreign protein particles or by disseminated intravascular coagulation from non-specific particles.

For our understanding of certain important biopharmaceutical and biological phenomena, the study of the particle-liquid interface and particle-particle interactions is essential. In many instances, the theory and its complicated mathematics have progressed further than its experimental proof. Indeed, there is an increasing need to determine and to interpret the kinetics, energetics and mechanism of interaction for real dispersions in liquid systems by the application of fundamental principles of physical chemistry.

LITERATURE REVIEW

This literature review emphasizes several biopharmaceutical and biological systems involving particles in liquids in which a basic understanding along a physico-chemical approach is needed.

Preferential Flocculation and Coalescence in Heterodispersed Systems

There are many situations involving suspensions and emulsions where with time the particles or droplets of the dispersed phase simultaneously increase in size and narrow in their relative size distributions, and then later become quite stable kinetically. If the dispersed phase is soluble (miscible) enough in the solvent, then the phenomenon may be accounted for by molecular diffusion (1) or Ostwald ripening. However, there are many examples in the literature (2-4) where the changes appear to occur primarily through particle-particle aggregation or droplet-droplet coalescence.

During the course of the present studies, it was observed that urea-denatured ovalbumin aggregates precipitated in buffered saline near the isoelectric point are often made up of rather uniform particles of around one micron diameter (see section III). Sherman (2) found

that emulsions pass through an initial phase of rapid coalescence followed by a second period of slow coalescence, and then the emulsions became relatively stable. All of his emulsions showed a relatively narrow size distribution in the later stages. Wiley (3) and Gillespie (4) have also studied the problem of limited coalescence when droplets in oil-in-water emulsions are stabilized by finely divided particles.

On the basis of the Smoluchowski theory of flocculation (5), Van den Tempel (6) studied the coagulation of oil-in-water emulsions in which he considered the process to consist of two steps, i.e. flocculation and coalescence. The rate of flocculation was regarded as the collision rate of droplets to form doublets and the coalescence included the breaking of the film and formation of a single particle. In an unstable system, flocculation may be the rate-controlling step. In a critical review of the stability of dispersed systems, Voyutskii (7) pointed out that the stabilization of dilute oil-in-water emulsions is essentially due to the electrical double layer repulsion between the oil droplets and, to a less degree, to the presence of an adsorption-solvation layer forming a structural and mechanical barrier. Earlier, Verwey and Overbeek (8) explained the effects of the particle size and the potential energy of interaction between particles on the stability of colloidal systems.

To explain limited flocculation and coalescence, investigations, for the most part, have used expressions limited to cases involving potential energy barriers for particles of equal sizes (8) or for particles of different sizes in which the mean size is used (2). For particles of unequal sizes, equations for the repulsive potential energy (9) and the attractive potential energy without retardation factors (10) have been derived. However, the attractive potential energy for unequal sizes with retardation factors, which is physically more realistic, have not been considered.

Flocculation and Sedimentation Behavior of Biochemical Systems

In clinical biochemistry, protein flocculation reactions are used for detecting abnormal changes in protein composition of biologic fluids for the diagnosis of hepatocellular diseases and other inflammatory diseases, such as arthritis, endocarditis, malaria, bacterial infections, etc. (11-15). These diseases show gamma-globulin excess with or without alteration of the albumin-total globulin ratio. Three of the most widely used tests are the cephalin-cholesterol flocculation, thymol and zinc sulfate turbidity tests, which have easily observable, semi-quantitative results with abnormal sera but no pronounced effect on normal sera. Each test becomes positive, relative to arbitrary standards, in the presence of sufficient increases of gamma-globulin fraction, particularly if albumin is also reduced since it inhibits the

flocculation. Saifer (16) reviewed protein flocculation reactions, in general, from a physico-chemical point of view, emphasizing the electrical double layer theory. The mechanism of action has been studied by determining which electrophoretic serum fractions are involved in the reaction, either as active components or as inhibitors. During the test, proteins denaturation is believed to occur from x-ray diffraction studies.

The propensity of proteins to undergo gross physical and chemical changes by denaturation is realized in clinical biochemistry. This characteristic property is the basis for diagnostic procedures involving heat coagulation of proteins, such as the Weltmann coagulation band (17) technique and certain serum flocculation tests for cancer (18, 19, 20) based on sulfhydryl-dependent molecular protein aggregation.

The sedimentation rate of erythrocytes is another routine clinical in vitro test of diagnostic importance, which is not specific for any disease but indicates the presence or absence of an inflammatory process (21). Physico-chemical factors, such as the electrical charge on the surface of the blood cell, pH, temperature and adsorption of plasma proteins and drugs, have been recognized to affect the rate.

In the area of molecular disease, specifically the sickle cell disease (19), the flocculation behavior of the sickle cell hemoglobin and the cell itself have

been relatively unexplained. Harris (23) has accumulated and reviewed the extensive physical and chemical data of the sickling phenomena. In sickle cell anemia, the red blood cells, containing a predominance of hemoglobin S of about 80-100 per cent of the total hemoglobin, undergo sickling at normal venous oxygen tension as the result of tactoid formation of the hemoglobin. If smaller amounts of the hemoglobin are in the abnormal form, sickling does not normally occur in the blood but can be induced in vitro by exposing the cells to unphysiologically low oxygen tensions (i.e. sickle cell trait). Under these conditions, sickle cell anemia and trait can be determined by microscopic observation of the morphological changes of the erythrocyte. The various abnormal hemoglobin molecules differ from each other by a specific "sickle peptide" on the globin portion leading to differences in net charge between them. Consequently, their electrophoretic patterns are significant permitting the characterization of the sickle cell disease.

Because many disease states show altered plasma protein and red blood cell profiles, a quantitative physicochemical approach to the understanding of the mechanism of many laboratory diagnostic procedures appear to be necessary and may contribute to a more instructive interpretation of the test results leading to differential characterization of diseases. In this connection, the influence of protein-bound drugs on the diagnostic tests should also be rigorously studied.

Macroaggregates of Denatured Proteins

The fact that small particles are able to pass through the vascular system in the human body, the smallest capillaries being approximately 5μ diameter, suggests several medical applications in which fine particles may serve as vehicles for the transport of radiation, therapeutic or diagnostic agents to a particular location in the body. Medical researchers have developed the use of denatured protein particles complexed with radioisotopes to measure renal, liver, splenic and pulmonary blood flow (24-26). Several preparations, i.e., particular macroaggregates of denatured human serum albumin complex with ^{131}I, ^{125}I or ^{99m}Tc, are used for the rapid diagnosis and location of pulmonary embolism by scintillation scanning on the basis of differential filtration of tracer particles at the embolism site (27-29). They are usually prepared by heat denaturation of the albumin and pH adjustment to obtain colloidal particles from 10 to 50μ diameter. The particle size distribution and physical stability of the suspension are critical problems of this diagnostic product because very small particles will make the interpretation of lung scans more difficult and large particles will increase the probability of further capillary embolization.

Particulate Matter in Parenteral Solutions

The presence of particulate matter in parenteral solutions has been a problem ever since this route of

administration has been accepted (30). The present United States Pharmacopoeia XVII and National Formulary X provide no guidelines for tests and standards of clarity in parenteral solutions. In Australia, a definitive standard has been proposed whereby a solution is acceptable if the particle counts per ml. are less than $1000 \geq 2.0\ \mu$ diameter, $250 \geq 3.5\ \mu$, $100 \geq 5.0\ \mu$ and $25 \geq 10\ \mu$, irrespective of the nature of the particle (31). This standard is admittedly arbitrary since the answers to a series of fundamental questions -- How many particles, what size particles and what kind can be tolerated with safety in a parenteral solution? -- are complicated by such factors as:

1. The extremely low probability of eliminating particles perfectly on a commercial scale,
2. The state of the technology in pharmaceutical manufacturing and quality control,
3. The present uncertainty of the clinical effects of extraneous particles of all kinds,
4. The medical problem of long-term therapy involving a depleted patient receiving a voluminous supply of parenteral fluids,
5. The experimental difficulties in correlating size, number and type of particles with biological insult.

The need for more research is clear for the ultimate attainment of a well-defined standard for clarity.

From microscopic identifications Garvan and Gunner (32, 33) classified the particles found as metal, glass, fiber, chemical, fungi, rubber and miscellaneous (insect parts, starch granules, etc.). Adverse effects from the injection of particles are not easily demonstrated, but the evidences indicate that emboli, thrombi and granulomas are produced (33-36) and that episodes of disseminated intravascular coagulation are possible (37). A review of some methods for the examination of parenteral solutions and measurements of the particle size distributions by the Coulter Counter are given by Vessey and Kendall (28) and others (31, 38, 39).

STATEMENT OF THE PROBLEM

Our review of the literature has shown that very little quantitative and mechanistic attempts have been carried out in certain areas of the formation, growth, flocculation or coalescence behavior of particles in liquids of great importance in biopharmaceutics and biology. In this regard, the studies were carried out with the following objectives:

1. to review existing theories of flocculation behavior of particles dispersed in aqueous systems,
2. to extend the above theories to describe the simultaneous effects of particle size and surface potential on preferential flocculation and coalescence in heterodispersed systems,
3. to develop a relatively novel technique to follow the kinetics of particle flocculation,
4. to study the flocculation behavior of denatured proteins by using the above technique and to correlate the data quantitatively with theory, and

5. to carry out an exploratory and quantitative study of the problem of particulate matter in parenteral solutions.

Thus, this thesis emphasizes the development of critical and quantitative experimental methods as well as the development of necessary theory so that problems involving particle-particle interactions can be handled.

SECTION I

THEORIES OF FLOCCULATION

This section is a review of flocculation theories of dispersed systems in aqueous medium. Later, these theories will be applied to the situation involving preferential flocculation or coalescence in hetero-dispersed systems and to the kinetics of flocculation of denatured proteins.

Smoluchowski's Theory of Rapid Flocculation of Mono-dispersed Systems

Smoluchowski worked out a basic theory of flocculation of spherical particles of a colloidal suspension (5). When the aggregation is controlled by Brownian diffusion in the absence of a force field, the flocculation of a relatively monodispersed system is given by the kinetic expression for bimolecular collision,

$$\frac{dN_\infty}{dt} = -K_s N_\infty^2 \qquad \text{(Eq. 1)}$$

Where N_∞ is the number of particles of all sizes, K_s is the rate constant, and t the time. Upon integration a linear relationship of $1/N_\infty$ versus t with slope K_s is predicted. For this case, the rate constant

is:

$$K_s = \frac{4\pi DR}{W} \qquad \text{(Eq. 2)}$$

where D is the effective diffusion coefficient, R is the distance between centers of the particles as shown in Fig. 1, and W is the stability factor. Since the collision is considered to be irreversible in a force-free field, W = 1. By assuming the Stokes-Einstein relationship for translational diffusion, i.e.,

$$D = \frac{kT}{6\pi\mu a} \qquad \text{(Eq. 3)}$$

and the effective collision radius, R = 2a, where k is the Boltzmann constant, μ the viscosity of the medium, T the absolute temperature, and a the particle radius, the theoretical maximum rate constant becomes

$$K_s = \frac{4kT}{3\mu} \qquad \text{(Eq. 4)}$$

In aqueous systems at 30° C., the theoretical value of K_s is 5.6×10^{-12} cm.^{3} sec.$^{-1}$.

Rapid Flocculation of Heterodispersed Systems

As an initially monodispersed system rapidly flocculates, the degree of polydispersity increases. The effect is an increase in the rate of flocculation. Thus, Eq. 1 applies only to an early period of time in which the particulate system is still relatively monodispersed. Furthermore, the equation is probably

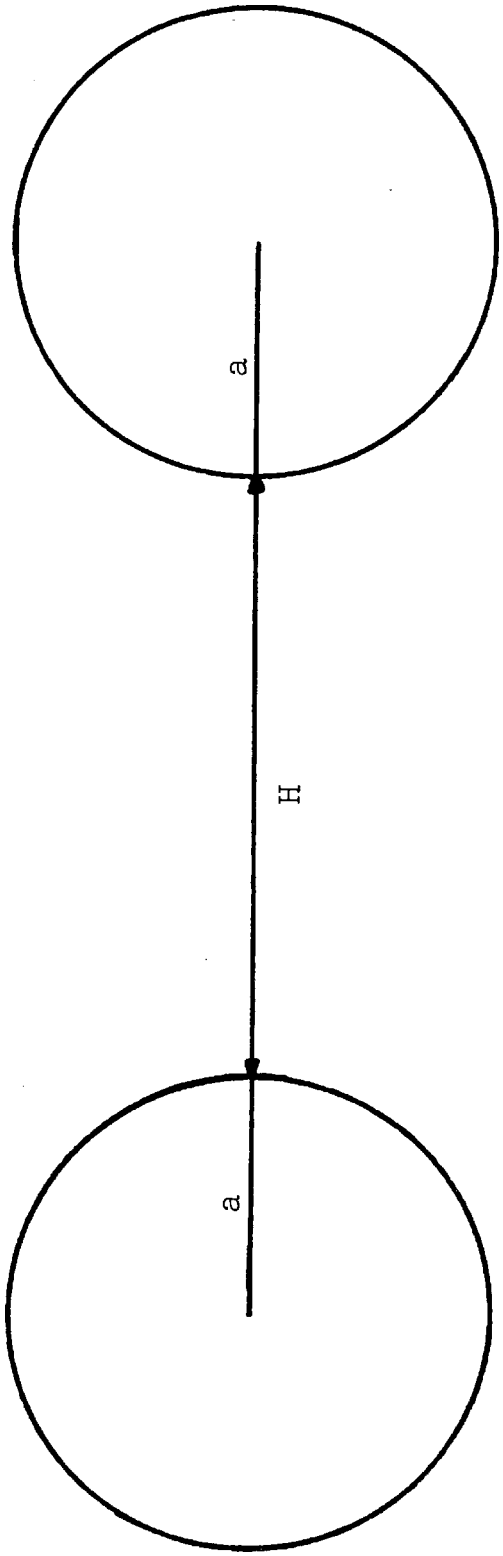

Figure 1. Geometrical consideration of two interacting spheres of equal radii, a. The radius of interaction is R = 2a + H where H is the shortest distance between the spheres.

a bad approximation for an initially, strong hetero-dispersed system.

Müller (40) explained these observations by the Smoluchowski theory for rapid flocculation. The rate of collision between spherical particles of sizes i and j is given by

$$G_{ij} = 4\pi D_{ij} R_{ij} n_i n_j \qquad \text{(Eq. 5)}$$

where G is the initial rate, D is the Stokes-Einstein diffusion coefficient, R is the distance between centers of two spheres in collision, and n is the concentration of particles. Also,

$$D_{ij} R_{ij} = \frac{kT}{6\pi\mu} \left(\frac{1}{a_i} + \frac{1}{a_j}\right) (a_i + a_j) \qquad \text{(Eq. 6)}$$

where k, T and μ are defined as before; consequently, the initial rate constant becomes

$$\text{Rate Constant} = \frac{2kT}{3\mu} \left(\frac{1}{a_i} + \frac{1}{a_j}\right) (a_i + a_j) \qquad \text{(Eq. 7)}$$

If the rate constant is plotted against the ratio of the particles sizes as shown in Fig. 2, one observes the preferential flocculation relationships due to Müller. When the ratio of the particle sizes is 10 to 1, the maximum limiting rate constant is about 3 times greater than that for particles of the same size. If the particles deviate markedly from the spherical form, the collision probability would be even greater.

General Particle Size Distribution Effects on the Rate of Flocculation

It has been pointed out that the assumption of

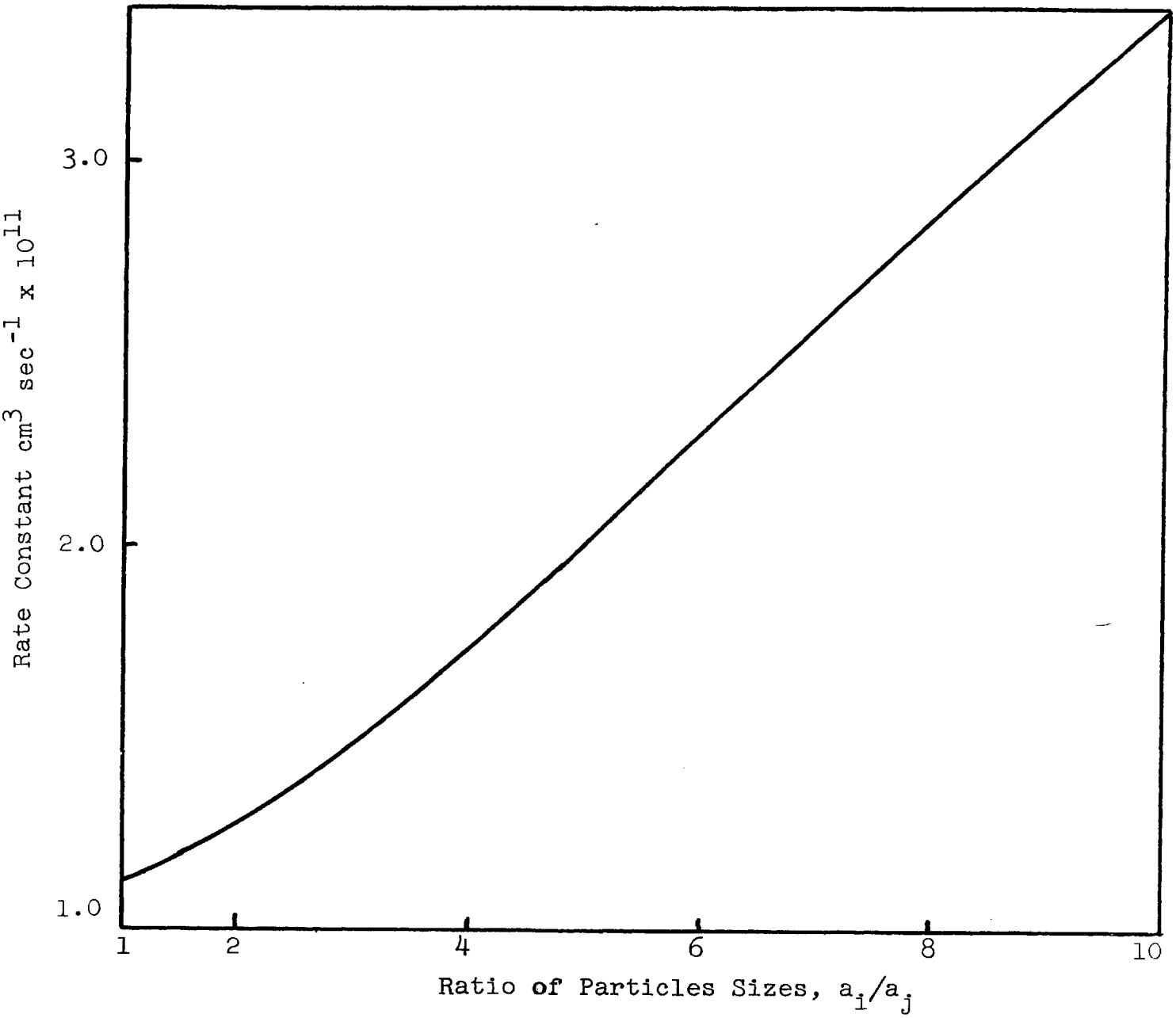

Figure 2. Probability of rapid flocculation between particles of different sizes when the stability factor W_{ij} equals unity.

uniform size distribution of particles limits the theory to the early stages of rapid, diffusion-controlled flocculation of a monodispersed system because of the inevitable broadening of the size distribution that follows. Müller's account of polydispersity is not widely applicable since it is limited to initial rates between two different monosized particle systems.

To completely describe the course of the flocculation process, Smoluchowski (5) derived the well-known fundamental equation of flocculation:

$$\frac{dn_k}{dt} = \frac{kT}{3\mu} \sum_{\substack{i=1 \\ j=k-i}}^{j=k-1} \left(\frac{1}{a_i} + \frac{1}{a_j}\right) (a_i + a_j)\, n_i n_j - \frac{2kT}{3\mu}\, n_k \sum_{i=1}^{\infty} \left(\frac{1}{a_i} + \frac{1}{a_k}\right) (a_i + a_k)\, n_i \qquad \text{(Eq. 8)}$$

This expression is a set of nonlinear ordinary differential equations which describes the rate of change of the concentration of particles of size n_k in a discrete distribution of particle sizes. The first term on the right of Eq. 8 represents the number of particles of size n_k formed by the flocculation of smaller particles, n_i and n_j, while the second term represents the number of particles of size n_k lost by flocculation with other particles. After summing over all sizes, the rate of change of the concentration of particles of the total size distribution, N_∞, becomes

$$\frac{dN_\infty}{dt} = d\frac{\sum_{k=1}^{\infty} n_k}{dt} = \frac{kT}{3\mu} \sum_{i=1}^{\infty} \sum_{j=1}^{\infty} \left(\frac{1}{a_i} + \frac{1}{a_j}\right) (a_i + a_j) n_i n_j \qquad \text{(Eq. 9)}$$

$$- \frac{2kT}{3\mu} \sum_{i=1}^{\infty} \sum_{k=1}^{\infty} \left(\frac{1}{a_i} + \frac{1}{a_k}\right) (a_i + a_k) n_i n_k$$

To provide an analytic solution to equations 8 and 9, Smoluchowski made the assumption that

$$\left(\frac{1}{a_i} + \frac{1}{a_j}\right) (a_i + a_j) \simeq 4 \qquad \text{(Eq. 10)}$$

which is applicable when the particles are all of the same size or relatively monosized. Upon applying this assumption to equation 9, the solution becomes identical to that of equation 1. In the limit that the particle system is initially of uniform size, Smoluchowski further showed that the solution of equation 8 was

$$n_k = \frac{n_o (t/\tau)^{k-1}}{(1 + t/\tau)^{k+1}} \qquad \text{(Eq. 11)}$$

where τ is the half-life,

$$\tau = \frac{3\mu}{4kTn_o} \qquad \text{(Eq. 12)}$$

and n_o is the initial particle concentration and k (subscript and superscript) = 1, 2, 3, etc. for the number of primary particles per aggregate.

Many attempts have been made to solve Smoluchowski's fundamental equation of flocculation. After transformation of the equation to the continuous size spectrum case, Martynov and Bakanov (41) suggested a general solution in the form of a power series, while Friedlander and Swift (42) utilized the self-preservation

hypothesis. Thereafter, Rice and Whitehead (43) worked out the exact solution for the discrete spectrum in a power series form and Hidy and Lilly (44,45) in the self-preservation form. In connection with equation 9, Gillespie (46) derived expressions for the rate constants for systems containing a distribution of particle sizes and showed that polydispersity increases the rate constant for diffusion-controlled collisions.

Similarity or Self-Preserving Theory of Flocculation

Friedlander and Swift (42) showed that certain forms of similarity or self-preserving functions can be applied to the solution of Smoluchowski's fundamental equation for flocculation. The relations depend upon the assumptions that the particle distribution in various sizes is continuous and that a particular form of the size spectrum is invariant with time. This leads to a transformation of the rate equation for a discrete spectrum to a nonlinear integro-differential equation for the rate of change of the concentration of particles over a size range of volume v to v + dv, although the latter model for the continuous spectrum is physically less realistic than the former.

In the theory of Friedlander and Swift the particle distribution is expressed as:

$$n(v,t) = \frac{N_\infty^{\,2}}{\phi} \quad \psi_1(\eta) \qquad \text{(Eq. 13)}$$

where $\psi_1(\eta)$ is a dimensionless distribution function,

the constant ϕ is the total volume fraction of particles:

$$\phi = \int_0^\infty vn(v)dv \qquad \text{(Eq. 14)}$$

and η is the dimensionless volume distribution:

$$\eta = \frac{vN_\infty}{\phi} \qquad \text{(Eq. 15)}$$

When $\eta = 1$, the average size of the particles with respect to volume is predicted. Furthermore,

$$N_v = N_\infty \int_\eta^\infty \psi_1(\eta)d\eta = N_\infty \psi_2(\eta) \qquad \text{(Eq. 16)}$$

where $\psi_2(\eta)$ is the dimensionless cumulative particle distribution. The term $n(v)dv$ is the number of particles between the sizes v and v + dv, N_v is the cumulative number of particles larger than v, N_∞ and t have been previously defined; ψ_1 and ψ_2 are time-independent functions and, therefore, do not depend upon the initial size distributions. The theory can be tested by plotting N_v/N_∞ versus η different time intervals. This plot should slow the tendency of the distribution to preserve its form and give ψ_2, the time-independent dimensionless cumulative distribution function, as predicted by equation 16.

According to the theory, if the $1/N_\infty$ versus t plot is linear, the rate of flocculation with the self-preserving size distribution can be described by:

$$\frac{dN_\infty}{dt} = \frac{-\alpha A_1 kTN_\infty^2}{3\mu} \qquad \text{(Eq. 17)}$$

where α is the collision efficiency having the same physical meaning as the factor W in Eq. 1, and

$$A_1 = [2 + 2\int_0^\infty \eta^{1/3}\, d\psi_2 \int_0^\infty \eta^{-1/3} d\psi_2] \qquad \text{(Eq. 18)}$$

When $\alpha = 1$ and $A_1 = 4.0$, the rate constant of Eq. 17 reduces to that of Eq. 2 for the homogeneous case, Thus A_1 is a significant parameter accounting for the effect of heterogeneity on the rate of flocculation. By comparing Eqs. 1 and 17

$$\alpha = \frac{3K_s\mu}{A_1 kT} = \frac{1}{W} \qquad \text{(Eq. 19)}$$

It should be noted that the approach of the self-preserving theory offers a method of determining the flocculation rate constant independent of that approach which assumed a relatively monodispersed system. Because it takes into account the size changes within a distribution with time, the theory can evaluate the factors of heterogeneity and collision efficiency influencing the flocculation process.

Slow Flocculation

The rate of slow flocculation depends upon the potential energy barrier between the particles. Fuchs (47, 48) treated this problem as diffusion of particles colliding in an electrical force field and found that the number of effective collisions was reduced by a factor of W. As previously stated, W is the stability factor. Between equal spheres, it is mathematically defined by the relationship,

$$W = 2a \int_{2a}^\infty \frac{\exp\,(V_T/kT)}{R^2}\, dR \qquad \text{(Eq. 20)}$$

where V_T is the total potential energy of interaction

which will be discussed later in Section II. Because W is a function of the particle size, it is not constant throughout the flocculation process. Therefore, equation 20, is an expression appropriate only to the retardation of flocculation of a monodispersed system in the early stages. To appreciably simplify the evaluation of the integral, Reerink and Overbeek (49) showed that W can be simply related to the maximum of the energy barrier,

$$W \sim \frac{1}{2Ka} \exp\left(V_{Tmax} / kT\right) \qquad \text{(Eq. 21)}$$

where K is the Debye-Huckel kappa. They also showed that the theory obeyed adequately the Schultz-Hardy rule for lyophobic colloids in aqueous systems.

When W is introduced into the diffusional flocculation rate equation, as in equations 1 and 17, the total potential energy of interaction, i.e. the combined effect of the repulsion by the electrical double layers and the attraction by Van der Waal forces, determines how fast the flocculation will proceed. One can approximate the value of W by two independent experimental methods and the appropriate theoretical equations: the first, being flocculation rate studies and the second involving the estimation of the surface potential by zeta potential measurements.

SECTION II

PREFERENTIAL FLOCCULATION AND COALESCENCE IN HETERODISPERSED SYSTEMS

It is the purpose of this section to examine the theory as it relates to preferential and limited flocculation (or coalescence). As will be seen, some of the theoretical conclusions consistently describe many of the findings of investigators in the field. Although the effects of the particle size on the stability of colloids have been recognized, quantitation has been limited to the case involving potential energy barriers for particles of equal sizes (8) or for particles of different sizes in which the mean size is used (2). While the equations for the repulsive potential energy between two unequal spheres have already been derived, an expression for the attractive potential energy between two unequal spheres with retardation factors has not been considered. This author is not aware of quantitative computations involving preferential collision of differing particle sizes in the presence of a repulsive barrier.

Theory

Rate of Preferential Aggregation or Coalescence

Let us assume that there are equal concentrations

of spherical particles of three sizes, that is, spheres S_1, S_2 and S_3 of radii a_1, a_2 and a_3 respectively, where $a_1 < a_2 < a_3$. The dispersion is in an electrolyte solution and the particles are allowed to aggregate (coalesce) at 25° C. The following question is asked: what are the probabilities of S_1 colliding with S_1, S_2 or S_3, of S_2 with S_2 or S_3 and of S_3 with S_3? By means of theory let us determine the initial rates of aggregation or coalescence for the various size pairs.

It will be assumed following the Dejaquin-Verwey-Overbeek concepts, the interparticle interaction results from electrical repulsion and the London-Van der Waals attraction. According to the theories of Smoluchowski and Fuch (5, 47), the rate of collision between spherical particles of sizes i and j is given by

$$G_{ij} = \frac{4\pi D_{ij} R_{ij} n_i n_j}{W_{ij}} \qquad \text{(Eq. 22)}$$

where G is the initial rate, D is the Stokes-Einstein diffusion coefficient, R is the distance between centers of the spheres, n is the concentration of particles and W is the stability factor. We may also write

$$D_{ij} R_{ij} = \frac{kT}{6\pi\mu} \left(\frac{1}{a_1} + \frac{1}{a_j}\right) (a_i + a_j) \qquad \text{(Eq. 23)}$$

where k is the Boltzman constant, T is the absolute temperature and μ is the viscosity of the suspending medium. Then the initial rate is

$$G_{ij} = \frac{2kT}{3\mu W_{ij}} \left(\frac{1}{a_i} + \frac{1}{a_j}\right) (a_i + a_j)\, n_i n_j \qquad \text{(Eq. 24)}$$

The factor W_{ij} accounts for the energy barrier to aggregation and is given by

$$W_{ij} = 2 \int_{2}^{\infty} \exp \left(\frac{V_{T(i,j)}}{kT}\right) \frac{ds}{s^2} \qquad \text{(Eq. 25)}$$

where $s = \frac{R}{\bar{a}}$ and $\bar{a} = \left(\frac{a_i + a_j}{2}\right)$. The W_{ij} usually ranges from $1 \lesssim W < \infty$ and takes into account the double layer potential, the concentration of electrolytes, London-Van der Waal dispersion forces and the particle sizes of the two spheres.

Potential Energy of Interaction

In Eq. 25 the $V_{T(i,j)}$ is the total potential energy of interaction between two particles and is given by the sum of the repulsive energy, $V_{R(i,j)}$, and the attraction energy, $V_{A(i,j)}$; thus

$$V_{T(i,j)} = V_{R(i,j)} + V_{A(i,j)} \qquad \text{(Eq. 26)}$$

The repulsive energy between interacting spheres of sizes i and j can be calculated by the approximate expression derived by Hogg, Healy and Fuerstenau (9).

$$V_{R(i,j)} = \frac{\varepsilon a_i a_j \psi_o^2}{(a_i + a_j)} \ln \left[1 + \exp(-KH)\right] \qquad \text{(Eq. 27)}$$

where ε is the dielectric constant of the medium, ψ_o is the surface potential, K is the reciprocal of the Debye-Huckel thickness of the double layer and H is the shortest distance between the surfaces of the spheres. The equation is valid for Ka_i and $Ka_j >> 1$. The quantity K is defined as:

$$K^2 = \left(\frac{4\pi e^2 \sum m_i Z_i^2}{\varepsilon kT}\right) \qquad \text{(Eq. 28)}$$

where e is the charge on the electron, m_i is the total number of ions per cm.^{3} of solution and Z_i is the valence of the ions.

The attraction energy of particles is more difficult to determine because the force between particles is considerably reduced by the retardation between atoms. Since the retardation effect is a function of distance, a single expression for the attraction energy is not available. When a_i, $a_j \gg H$ and $H \leq 150^{\circ}$ A, the attraction interaction energy can be calculated by the expression

$$V_{A(i,j)} = -\frac{Aa_ia_j}{6(a_i + a_j)H}\left(\frac{\lambda}{\lambda + 11.116\ H}\right) \qquad \text{(Eq. 29)}$$

where A is the Hamaker constant and λ is the characteristic wavelength of the atoms.

For $H \gtrsim 150^{\circ}$ A,

$$V_{A(i,j)} = \frac{Aa_ia_j}{(a_i + a_j)}\left[\frac{-2.45\lambda}{60\pi H^2} + \frac{2.17\lambda^2}{360\pi^2 H^3} - \frac{0.59\lambda^3}{1680\pi^3 H^4}\right] \qquad \text{(Eq. 30)}$$

One should refer to the Appendix I for the discussion of the retardation factor and the derivation of equations 29 and 30 and also to Appendix II for further discussion of the potential energy of repulsion between unequal spheres. For situations where a sphere may be interacting with an infinitely long flat plate, perhaps in the case of micellar transport of drugs to the intestinal wall, expressions have been derived in Appendix III for the retarded attractive and repulsive interaction energies.

Calculations

Computations employing equations 24-30 were carried out for a wide range of conditions with the aid of the IBM 7090 Digital Computer. ψ_o values from 0 to 100 mv and various radius combinations were taken at different K (see Table I). Because the Hamaker constant is estimated (50-52) to be somewhere in the neighborhood of 1 to 5 X 10^{-13} erg for most organic substances in water, calculations were made using the two values, 1 X 10^{-13} and 5 X 10^{-13}. The characteristic wavelength, λ, has taken to be 10^{-5} cm. Some plots of V_T vs. H are shown in Fig. 3-5.

Table II presents some of the significant results. Calculated values of V_{Tmax}, the maximum in the V_T vs. H curves, are shown. The rate constant, G', is defined as

$$G' = \frac{G_{ij}}{n_i n_j} \qquad \text{(Eq. 31)}$$

Discussion

When K is large, i.e. $K \gtrsim 0.4$ to 2 X 10^7, or when $\psi_o \simeq 0$, it is seen (Table II) that, for essentially all particle sizes in the range of 0.1 to 5.0 μ radius, the rates of aggregation approach the Smoluchowski rates. Thus, in aqueous 1% NaCl solutions, maximum rates may be expected. Under these conditions for which W_{ij} equals unity[1], the well-known preferential aggregation

---

[1]Actually the limiting W_{ij} values may be somewhat less than unity when all repulsive barriers are removed because V_T will be negative (See Eq. 25).

relationship due to Müller (See Section I) can be seen here. However, under such "rapid" aggregation conditions, the rate constant for a 0.1 μ - 1.0 μ pair is only 3 times greater than that for particles of the same size.

Let us now direct our attention to the region of kinetic stability where the rates may be regarded as neither very rapid or very slow. In this intermediate stability region we note a dramatic change in importance of particle size. This can be seen in Table II and in Figure 6. In Figure 6, it can be seen how electrolyte concentration may markedly increase the preference for the aggregation (or coalescence) of small particles with each other or with large particles. Thus, when $K \simeq 2$ to 4×10^6 for $\psi_o \simeq 25$ mv it can be seen (Table II or Fig. 6) that the rate of aggregation (or coalescence) of 0.1 μ particles with itself or larger particles may be 10 to 30 orders of magnitude greater than that for two 0.5 μ particles. Comparing Fig. 6 with Fig. 7, we note that the rates for various particle sizes are highly sensitive to the Hamaker constant taken as 1×10^{-13} and 5×10^{-13} erg.

The above conclusions depend upon the assumption that other contributions to particle-particle repulsion are absent. Therefore, in the case of emulsion-coalescence, strongly adsorbed barriers forming interfacial films are absent. In practice

TABLE I

Relationship between the Debye-Huckel K and the Electrolyte Concentration

K, cm^{-1}	Double layer thickness 1/K in ^{o}A	% NaCl
2×10^{6}	50	0.02
4×10^{6}	25	0.09
1×10^{7}	10	0.6
2×10^{7}	5	2.2

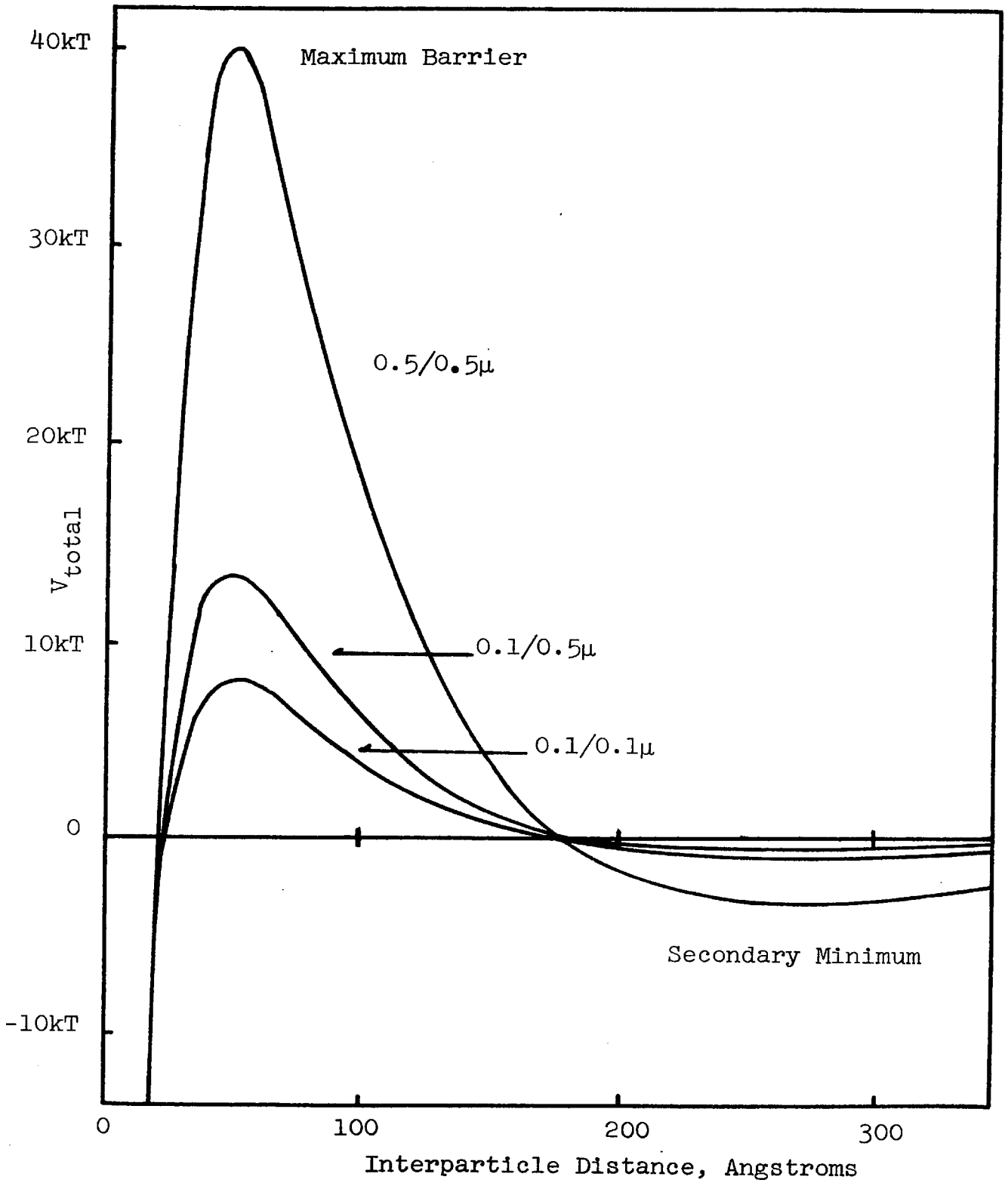

Figure 3. Influence of particle sizes on the total potential energy of interaction. $A = 5 \times 10^{-13}$ ergs, $\psi_o = 25$ mv and $K = 2 \times 10^6$ cm^{-1}.

Figure 4. Influence of electrolyte concentration on the total potential energy of interaction for two particle sizes. $A = 1 \times 10^{-13}$ ergs and $\psi_o = 25$ mv.

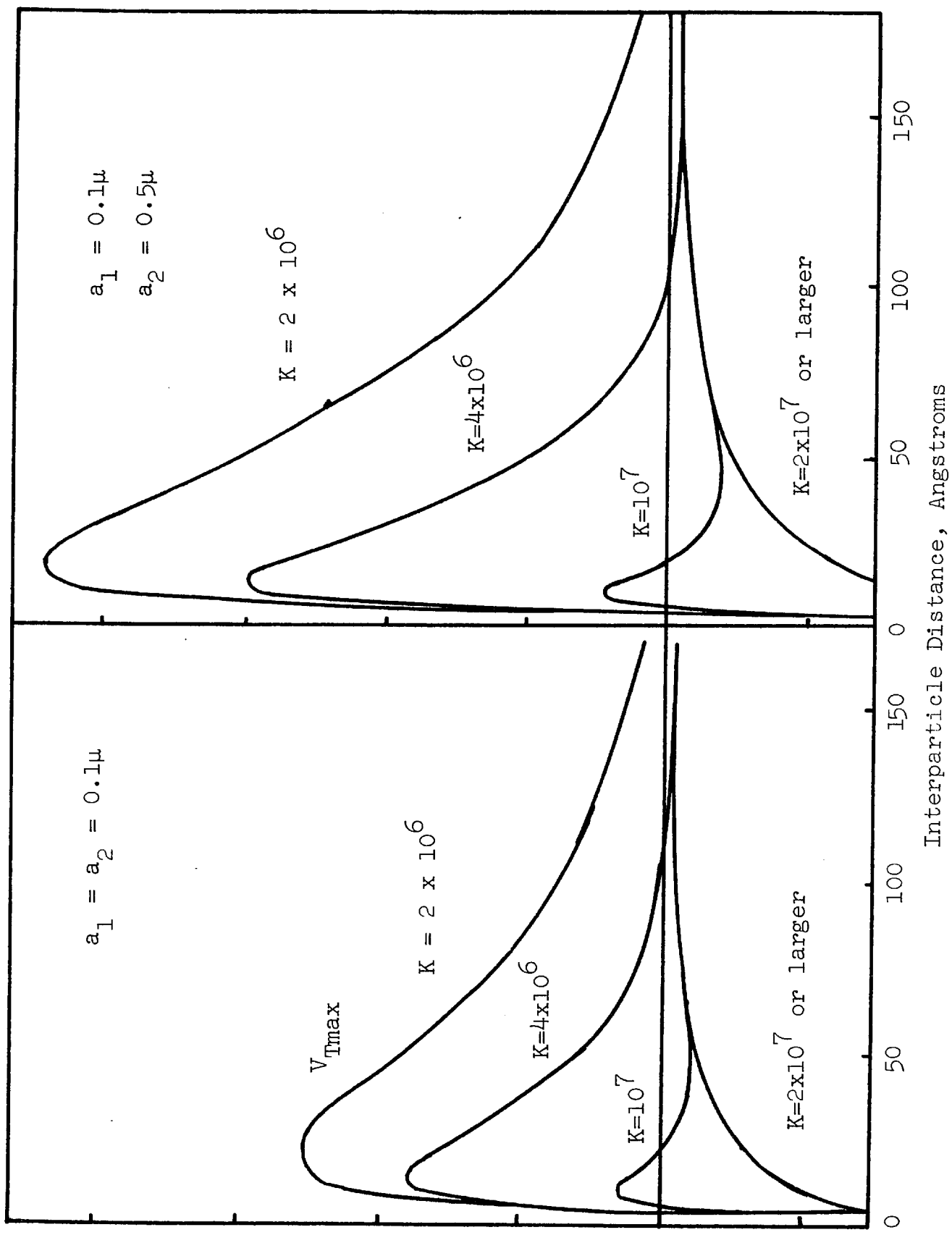
$a_1 = a_2 = 0.1\mu$
V_{Tmax}
K = 2 x 10^6
K=4x10^6
K=10^7
K=2x10^7 or larger
a_1 = 0.1μ
a_2 = 0.5μ
K = 2 x 10^6
K=4x10^6
K=10^7
K=2x10^7 or larger
40kT
30kT
20kT
10kT
0
-10kT
V_{total}
0
50
100
150
0
50
100
150
Interparticle Distance, Angstroms

Figure 5. Influence of surface potential on the total potential energy of interaction for two particle sizes. $A = 5 \times 10^{-13}$ ergs, and $K = 2 \times 10^{6}$ cm^{-1}.

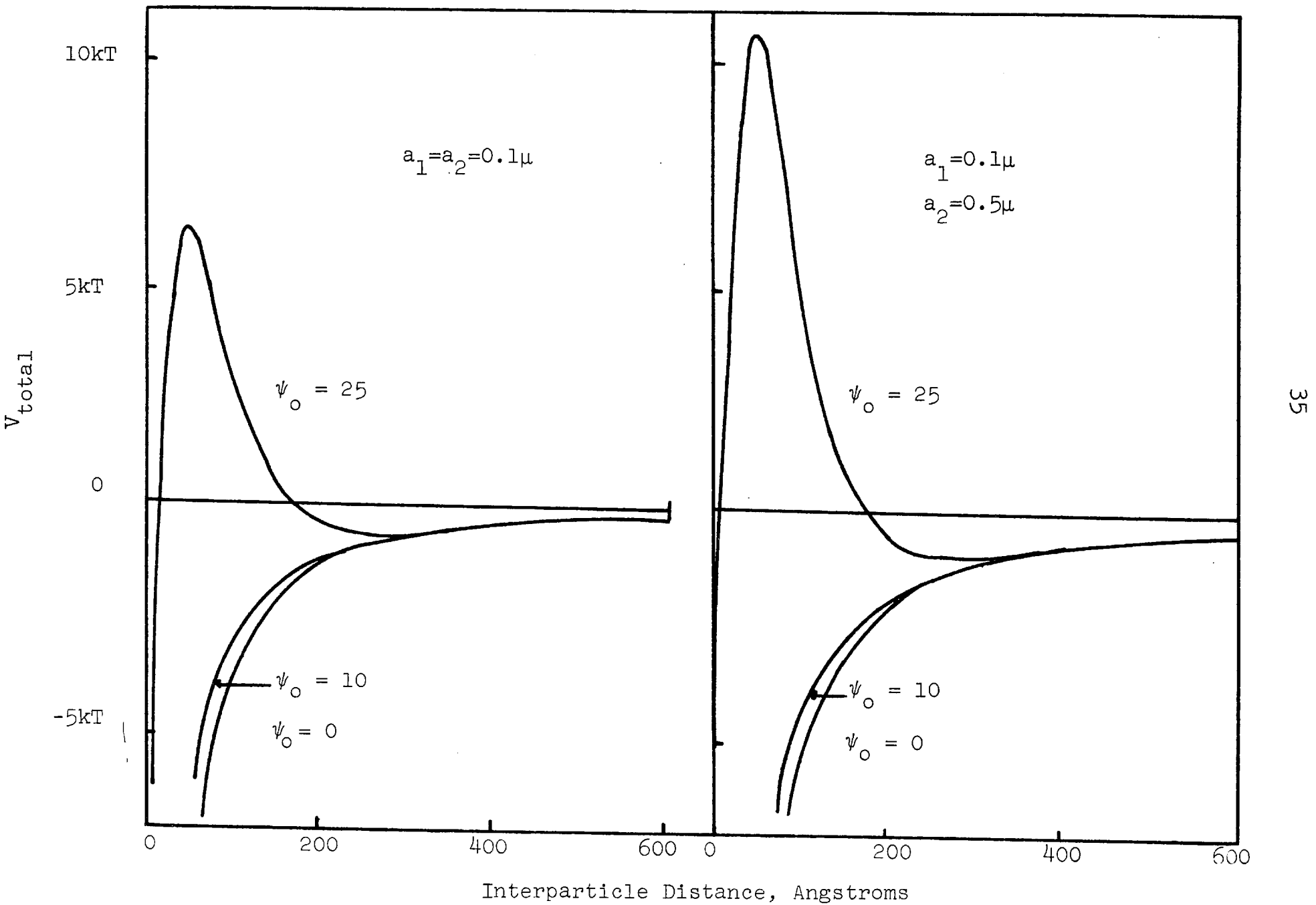
10kT
5kT
0
-5kT
V_{total}
$a_1=a_2=0.1\mu$
$\psi_o = 25$
$\psi_o = 10$
$\psi_o = 0$
$a_1=0.1\mu$
$a_2=0.5\mu$
$\psi_o = 25$
$\psi_o = 10$
$\psi_o = 0$
0
200
400
600
0
200
400
600
Interparticle Distance, Angstroms

Table II. Summary of data on the influence of electrolyte concentration (K), surface potential (ψ_o) and the Hamaker constant (A) on the maximum potential interaction energy of the barrier (V_{Tmax}) and the rate constant for flocculation (G').

A ergs	ψ_o mv	K cm^{-1}	Radii 0.1 and 0.1μ		Radii 0.1 and 0.5μ		Radii 0.1 and 1.0μ	
			G'	V_{Tmax}/kT	G'	V_{Tmax}/kT	G'	V_{Tmax}/kT
1×10^{-13}	0	———	11.2×10^{-12}	~0	20.2×10^{-12}	~0	33.9×10^{-12}	~0
	10	2×10^6	5.2×10^{-12}	0.77	5.6×10^{-12}	1.28	8.4×10^{-12}	1.40
		$\geq 4 \times 10^6$	11.2×10^{-12}	~0	20.2×10^{-12}	~0	33.9×10^{-12}	~0
	25	2×10^6	3.0×10^{-24}	25.73	5.8×10^{-28}	42.88	3.6×10^{-29}	46.78
		4×10^6	2.4×10^{-17}	17.43	1.2×10^{-21}	29.05	3.6×10^{-22}	31.69
		1×10^7	8.6×10^{-13}	2.56	2.8×10^{-13}	4.26	3.1×10^{-13}	4.65
		$\geq 2 \times 10^7$	11.2×10^{-12}	~0	20.2×10^{-12}	~0	33.9×10^{-12}	~0
5×10^{-13}	0	———	11.2×10^{-12}	~0	20.2×10^{-12}	~0	33.9×10^{-12}	~0
	10	$\geq 2 \times 10^6$	11.2×10^{-12}	~0	20.2×10^{-12}	~0	33.9×10^{-12}	~0
	25	2×10^6	19.4×10^{-14}	7.75	6.0×10^{-15}	12.91	5.7×10^{-15}	14.08
		$\geq 4 \times 10^6$	11.2×10^{-12}	~0	20.2×10^{-12}	~0	33.9×10^{-12}	~0

Table II (continued)

A ergs	ψ_o mv	K cm^{-1}	Radii 0.5 and 0.5μ G'	Radii 0.5 and 0.5μ $V_{Tmax/kT}$	Radii 0.5 and 1.0μ G'	Radii 0.5 and 1.0μ $V_{Tmax/kT}$	Radii 1.0 and 1.0μ G'	Radii 1.0 and 1.0μ $V_{Tmax/kT}$
1×10^{-13}	0	———	11.2×10^{-12}	~0	12.6×10^{-12}	~0	11.2×10^{-12}	~0
	10	2×10^6	2.4×10^{-13}	3.84	7.6×10^{-14}	5.11	5.2×10^{-15}	7.67
		$\geq 4 \times 10^6$	11.2×10^{-12}	~0	12.6×10^{-12}	~0	11.2×10^{-12}	~0
	25	2×10^6	1.1×10^{-65}	129.63	$<<10^{-65}$	171.51	*	257.27
		4×10^6	6.3×10^{-47}	87.15	$<<10^{-47}$	116.20	*	174.29
		1×10^7	3.1×10^{-15}	12.79	7.4×10^{-16}	17.05	1.7×10^{-19}	25.58
		$\geq 2 \times 10^7$	11.2×10^{-12}	~0	12.6×10^{-12}	~0	11.2×10^{-12}	~0
5×10^{-13}	0	———	11.2×10^{-12}	~0	12.6×10^{-12}	~0	11.2×10^{-12}	~0
	10	$\geq 2 \times 10^6$	11.2×10^{-12}	~0	12.6×10^{-12}	~0	11.2×10^{-12}	~0
	25	2×10^6	3.4×10^{-26}	38.73	1.41×10^{-31}	51.62	1.1×10^{-42}	77.46
		$\geq 4 \times 10^6$	11.2×10^{-12}	~0	12.6×10^{-12}	~0	11.2×10^{-12}	~0

* Rate constant is negligible
Note that when $V_{Tmax/kT} > 0$, little repulsive barrier exists, hence flocculation is dependent on the London van der Waal attraction.

Figure 6. Rate constant (G') as a function of concentration of 1-1 electrolyte for various particle sizes. $A = 1 \times 10^{-13}$ ergs and $\psi_o = 25$ mv.

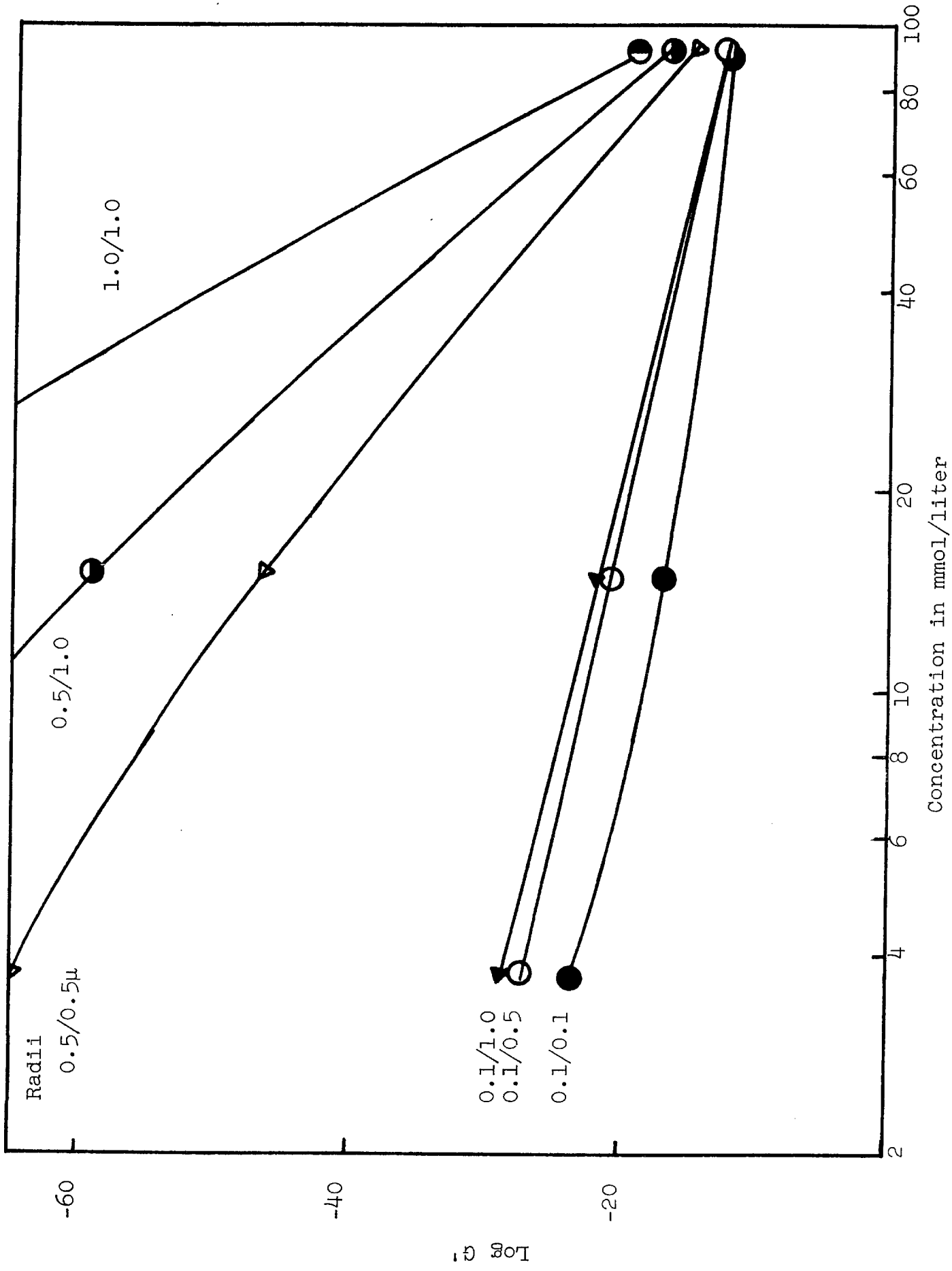
Log σ'
-60
-40
-20
2
4
6
8
10
20
40
60
80
100
Concentration in mmol/liter
1.0/1.0
0.5/1.0
Radii
0.5/0.5μ
0.1/1.0
0.1/0.5
0.1/0.1

Figure 7. Rate constant (G') as a function of concentration of 1-1 electrolyte for various particle sizes. $A = 5 \times 10^{-13}$ ergs and $\psi_o = 25$ mv.

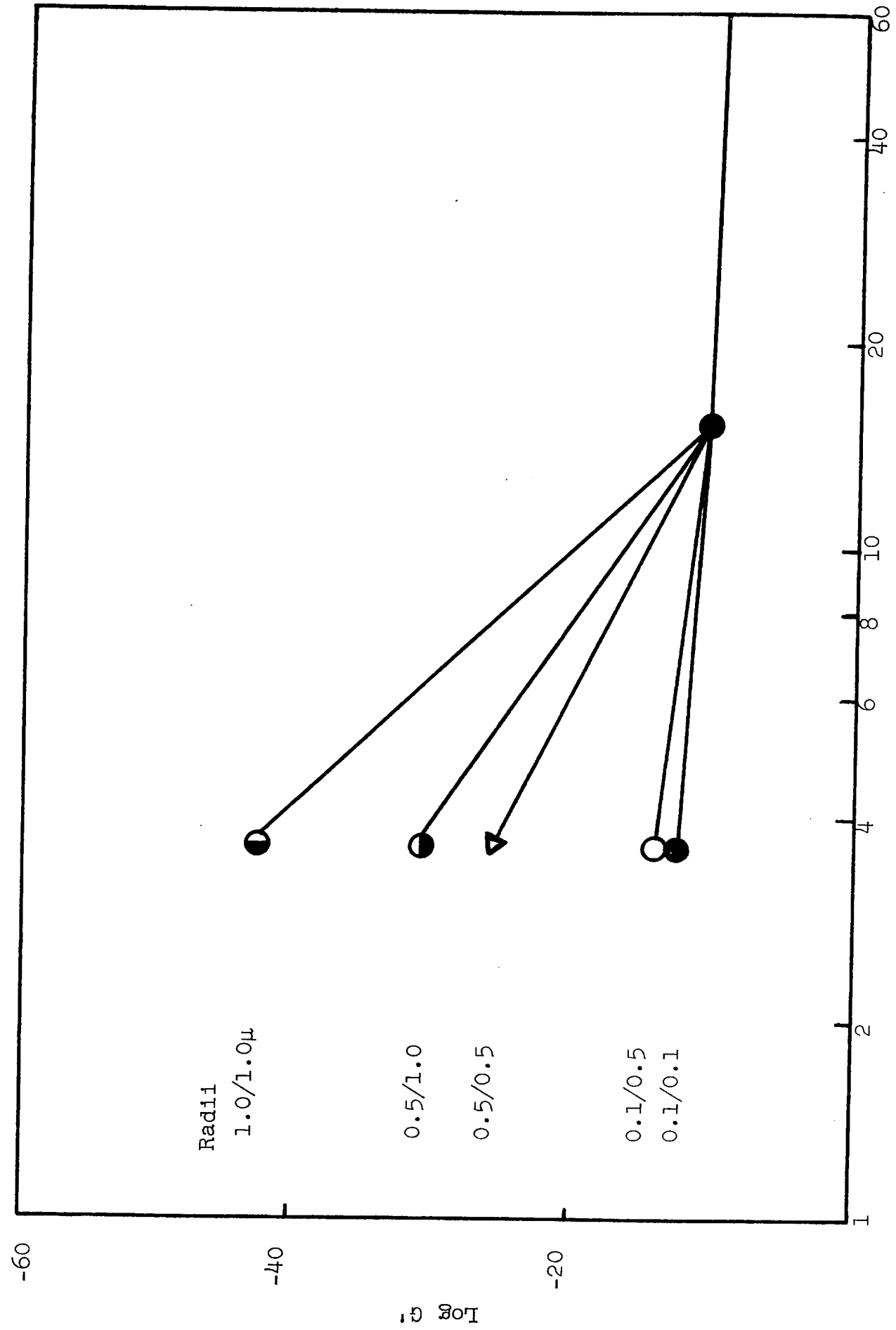
Radii
1.0/1.0μ
0.5/1.0
0.5/0.5
0.1/0.5
0.1/0.1
-60
-40
-20
Log σ'
1
2
4
6
8
10
20
40
60
Concentration in mmol/liter

one would expect that when surface coverage of ionic emulsifiers is low, say about 5 to 10% of maximum coverage, the repulsion between two oil droplets in an aqueous medium would be primarily electrical. These findings are consistent with the observations (2) that there is frequently an initial period of rapid coalescence with freshly prepared emulsions. Usually this is explained on the basis of the lack of sufficient stabilizer to provide a complete monolayer for the droplets. However, this explanation alone does not account for the relatively narrow size distributions that often result. The absence of small particles indicates that they preferentially disappear rapidly.

It is proposed that in a freshly prepared emulsion the shortage of surfactant prevents the formation of complete interfacial adsorbed films. Consequently, the rupture or displacement of the adsorbed molecules may not be rate determining in coalescence. Then if ψ_o is low ($\lesssim$ 25 mv) or if K is large, the rapid and selective disappearance of small droplets through coalescence would occur. The surviving larger droplets coalesce at a much slower rate as W_{ij} is extremely sensitive to particle size. Thus, a relatively narrow distribution would result if Brownian motion alone is inducing the coalescence.

Gillespie (4) has discussed limited coalescence of oil-in-water emulsions stabilized by finely divided

solids. He proposed a theory based on the rate of accretion of the solid stabilizer by the oil droplets. Furthermore, he found that there was an optimum concentration range for an ionic surfactant additive that produced the most uniform stable drops. This concentration range of the ionic surfactant appeared to produce a moderate or small electrical repulsive barrier. These findings are consistent with our theoretical results.

While the findings are only tentative, the precipitation of denatured proteins near the isoelectric point appears to involve the formation of relatively uniform primary particles of around one micron diameter (See Section III). Such narrow distributions are consistent with the above theory that selective flocculation of small particles with large ones take place. The extreme situation where only single denatured protein molecules deposit upon the larger particles would lead to the formation of relatively compact spherical particles of relatively narrow size ranges.

This author believes that the results presented provide a much better understanding of the role of particle size in the mechanisms of aggregation and coalescence. It provides a possible scientific basis for tailor-making dispersion formulations of controlled size and size distributions.

SECTION III

KINETICS OF FLOCCULATION OF DENATURED PROTEINS

While the protein chemists have intensified their investigations on the denatured protein mainly in the direction to unravel the structure of the native protein and to study the kinetics, mechanisms, and energetics of the denaturation process itself, the kinetics of growth and flocculation of denatured protein particles has received little or no attention. Research on the particulate behavior of denatured proteins should contribute to the fundamental understanding of the techniques in clinical laboratory procedures involving sedimentation of denatured proteins and in the interpretation of relevant data. This could also be extended to the understanding of blood cell and other protein flocculation reactions of biochemical importance.

In the field of applied pharmaceutical chemistry, such studies should provide a basic approach to the preparation of protein particles tagged with radioactive substances for the rapid diagnosis of embolism. Through the application of controlled growth and flocculation, one should be able to "tailor-make" a stable denatured protein particle or aggregate of uniform and

desired size.

The long range objective of research would be to study the kinetics of growth and flocculation of denatured protein particles on a quantitative basis in which the effects of protein species and concentration, the method of denaturation, pH, temperature, mono- and polyvalent electrolytes, solvents and surface-active agents are examined. The purpose of this section is to present a well-defined procedure for carrying out such studies. It involves the use of an electronic resistance counter with a multichannel particle size analyzer to follow changes in particle size distributions with time. For the model system studied here, the urea-pH induced denaturation of ovalbumin (53) was chosen taking advantage of the well-defined properties and the better controlled irreversible denaturation of ovalbumin.

Experimental

Materials and Method of Denaturation

A single lot of twice crystallized, lyophillized ovalbumin[2] was used throughout the study without further recrystallization and stored in a tight container under refrigeration to maintain stability of the protein. Urea used was reagent grade. Buffer solutions were prepared from reagent grade salts and standardized with the Beckman zeromatic pH meter.

---

[2]Worthington Biochemical Corp., Freehold, N. J.

One-half and 1% ovalbumin solutions in 8 M urea-phosphate buffer were prepared in the following manner. Ovalbumin was dissolved in a small amount of 0.05 M phosphate buffer (pH 6.88 and previously filtered through 0.45 μ Millipore filters) without stirring. To this was added the freshly prepared phosphate buffered urea solution with gentle stirring. The final pH was 7.1. Denaturation of the protein was carried out at constant stirring of 20 r.p.m. with a synchronous motor and in a closed system thermostated at 30°. At the end of 5 days, the denatured protein solution was discarded to avoid the complications of cyanate formation from the alkaline hydrolysis of urea (54).

Procedure for Flocculation Studies

Samples of the urea-denatured ovalbumin were used for the flocculation experiments after the viscosities of the solutions became constant. The viscosities were followed with an Ostwald viscometer. After denaturation periods of at least 18 hr., the protein solutions were diluted into 0.01 M acetate-normal saline buffer solutions, previously adjusted to pH 4.6 or 5.5, so that the final concentration was 1 mcg. denatured protein per ml. Also, normal saline adjusted to pH 8.7 with sodium hydroxide was used as a diluting solution. Initially, the solutions were mixed with gentle stirring and then allowed to stand without disturbance. Dilutions were made for several denaturation periods.

The course of the flocculation with time was followed by the single channel Coulter counter, model A, and the RIDL multichannel particle analyzer. Both the 30-μ and 50-μ aperture tubes were used. For the counting runs, a further 1:11 dilution of the master suspension was necessary to minimize coincidence errors. The initial particle concentrations were in the neighborhood of 1×10^7 particles per ml. Since the flocculating system was somewhat sensitive to the method of dilution, a procedure was developed that did not influence the results. A 1-ml. transfer pipet, Kimax -51 No. 37034-A, blow-out type, was used to pipet and deliver an aliquot at the rate of 1 ml./15 sec. The delivery was performed with the tip of the pipet under the surface of the diluting medium and the remaining drops were gently blown out. The samples were then immediately counted.

Particle Counter and Size Analyzer System and Its Standardization

To follow flocculation, changes in the particle size distribution as a function of time were followed by a new electronic resistance counter system shown schematically in Fig. 8. The system consists of a particle detector apparatus based on the Coulter counter[3] principle and a sophisticated transistorized RIDL 400 channel analyzer[4], which was originally developed for

[3] Coulter Electronics, Franklin Park, Illinois.

[4] Radiation Instrument Development Laboratory, Inc., Melrose Park, Illinois.

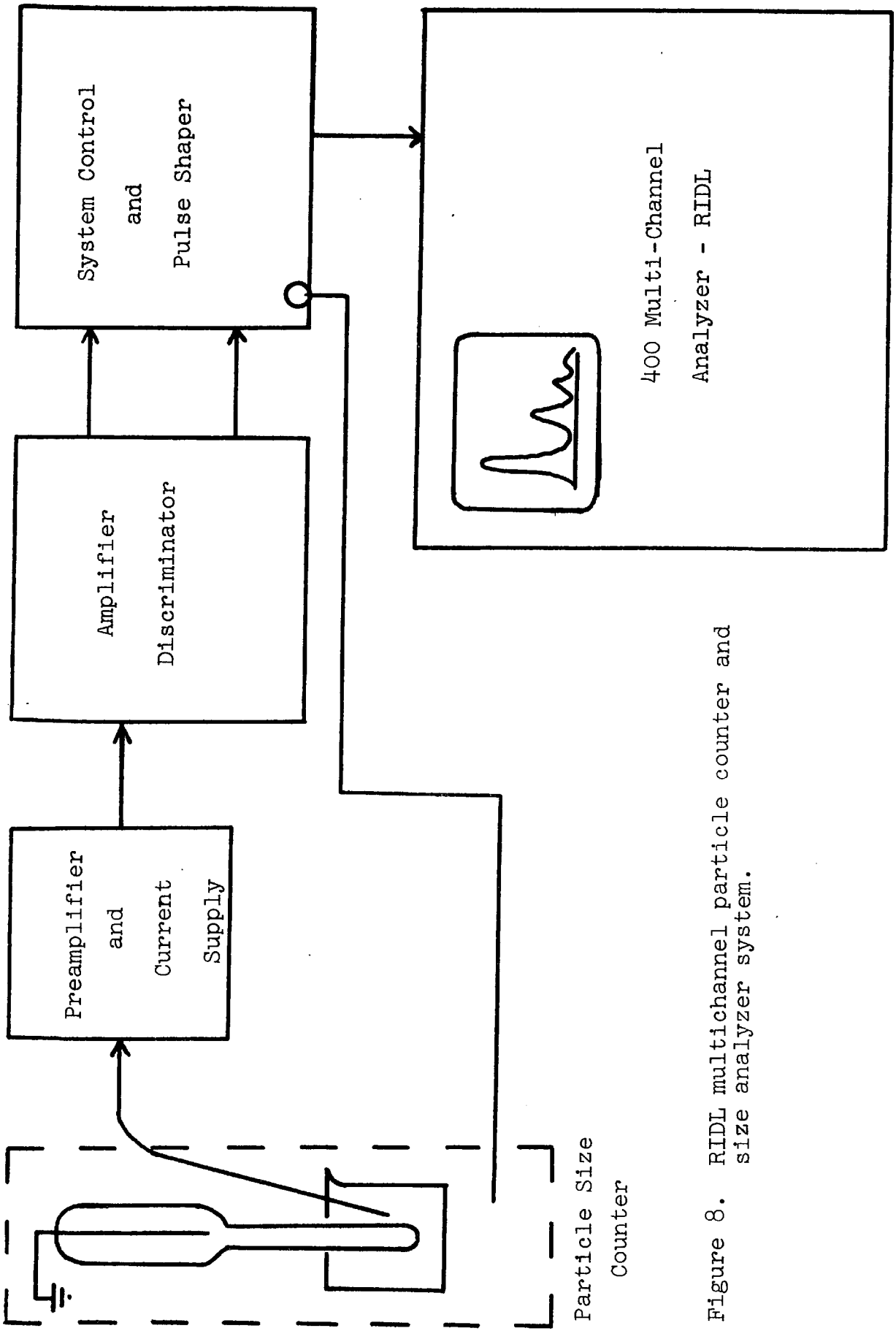

Figure 8. RIDL multichannel particle counter and size analyzer system.

γ-ray spectrometry. A constant current is supplied to the aperture tube of the detector apparatus. As a particle moves through the aperture, there is an abrupt change in the aperture current. The current signal is amplified and converted to a voltage pulse by the preamplifier. The pulse is then shaped and sent on to the pulse height analyzer where is is classified into one of the 400 channels and counted. Only one pulse can be analyzed at a time, but the analyzer performs this task in the order of milliseconds before accepting another pulse.

The distribution of particle size densities can be oscillographically displayed or stored in memory. By utilizing only 100 channels at a time, it is possible to simultaneously hold in memory up to four particle size distributions which may be displayed independently or simultaneously on the oscilloscope screen. Corrections for background may also be programmed.

While in most of the present work the data were presented on the oscilloscope screen and photographed with a Polaroid camera, other convenient modes of data retrieval may be used. Numerical readout devices and conventional recorders are easily adapted to the instrument.

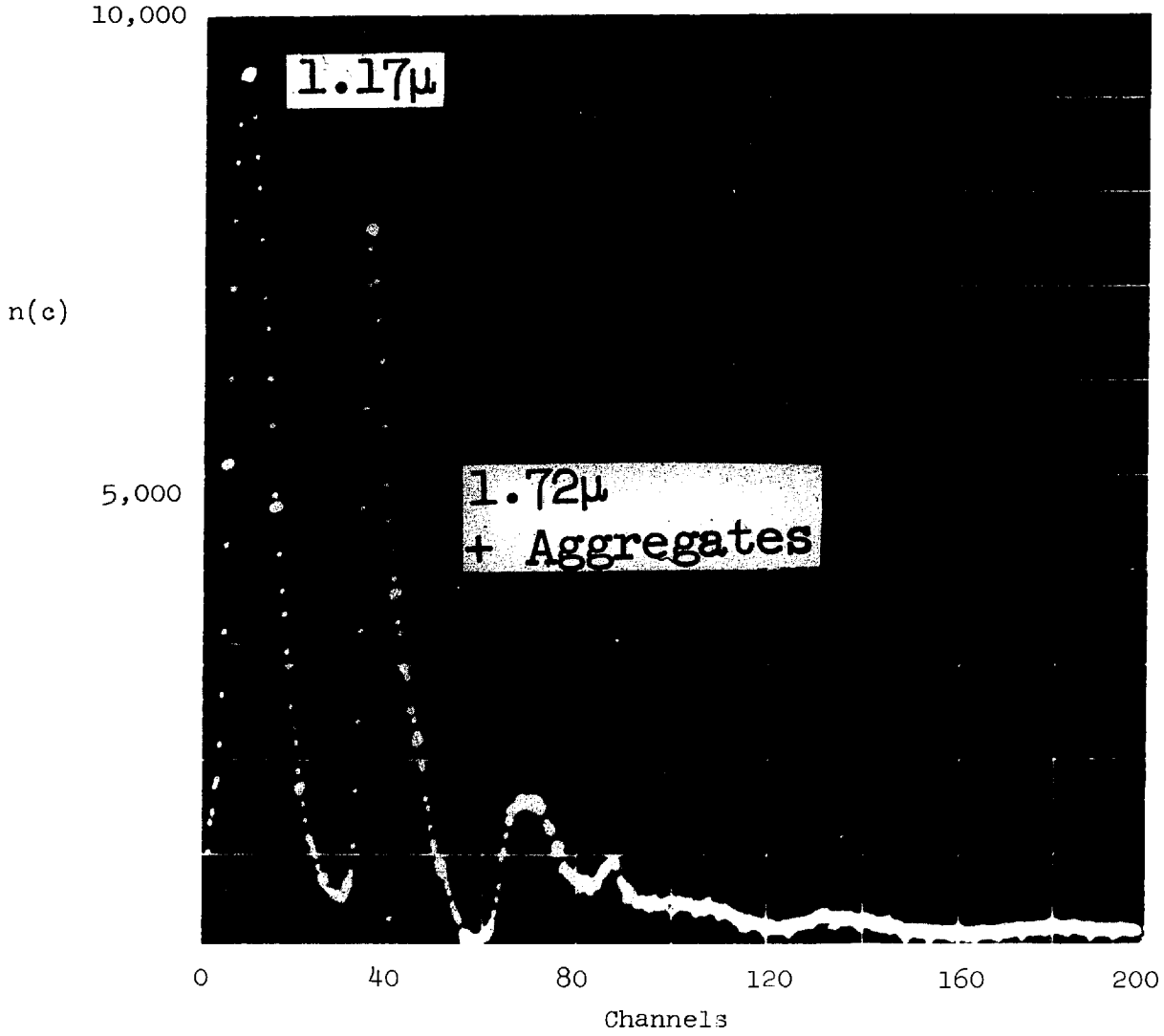

Figure 9. Differential distribution data for a mixture of 1.17 and 1.72-μ diameter latices. Two-hundred channels used. n(c) is the concentration of particles in channel c.

Standardization of the multichannel particle analyzer was accomplished with 1.17, 1.72, and 2.051-μ diameter polyvinyltoluene latices[5] suspended in 0.90% sodium chloride solutions. All of the standard lactices were washed repeatedly with alcohol and water by centrifugation, and the latter two latices were aggregated to some degree with magnesium sulfate. Microscopic measurements and the Coulter counter, model A, served as a check. Figure 9 shows the differential distribution of a mixture of 1.17-μ and aggregated 1.72-μ diameter latices. It is the oscillographic spectrum actually displayed by the 400 multichannel analyzer. Here, however, only 200 channels have been used to describe the distribution. The channel number is proportional to particle volume and the x-axis is calibrated with at least two known standards. The total number of particles corresponding to a given channel is represented by a point so that there will be as many points on the smooth distribution curve as there are preselected number of channels. At the 10th channel in Fig. 9, there is essentially a unimodal distribution of the 1.17-μ particles. The sharp singlet peak for the 1.72-μ particles occurs at approximately the 35th channel, and the triplet aggregate at the 105th channel as expected. However, there is in addition an odd

---

[5]Dow Chemical Co., Midland, Michigan.

small peak at the 90th channel.[6] The somewhat broader distributions of the high order aggregates are probably due to the wider distributions of shapes (configurations). The distribution of the 1.72-μ latices shows about 45% aggregation. When longer sampling times were taken, the statistics for the higher order aggregates improved and even 8-mers were detectable for the 1.72-μ aggregated system at approximately the 285th channel. There is relatively good linearity with this system. Figure 10

---

[6] Tentatively, this author has assigned both peaks at the 90th and 105th channels to triplet aggregates. Microscopically, the triplet aggregates appear in three general geometrical forms, viz., the triangular, linear, and other angular arrangements. According to rough theoretical calculations on the effect of particle shape factors on the electronic particle detection system and qualitative experimental data on the rearrangement kinetics of the triplet aggregates, there would be approximately a spread of 10 to 20 channels between the more stable triangular triplet aggregate and the other triplet aggregates. To some extent, Kubitschek (55) discussed the effect of shapes on electronic measurement of particle sizes. This study is being pursued further.

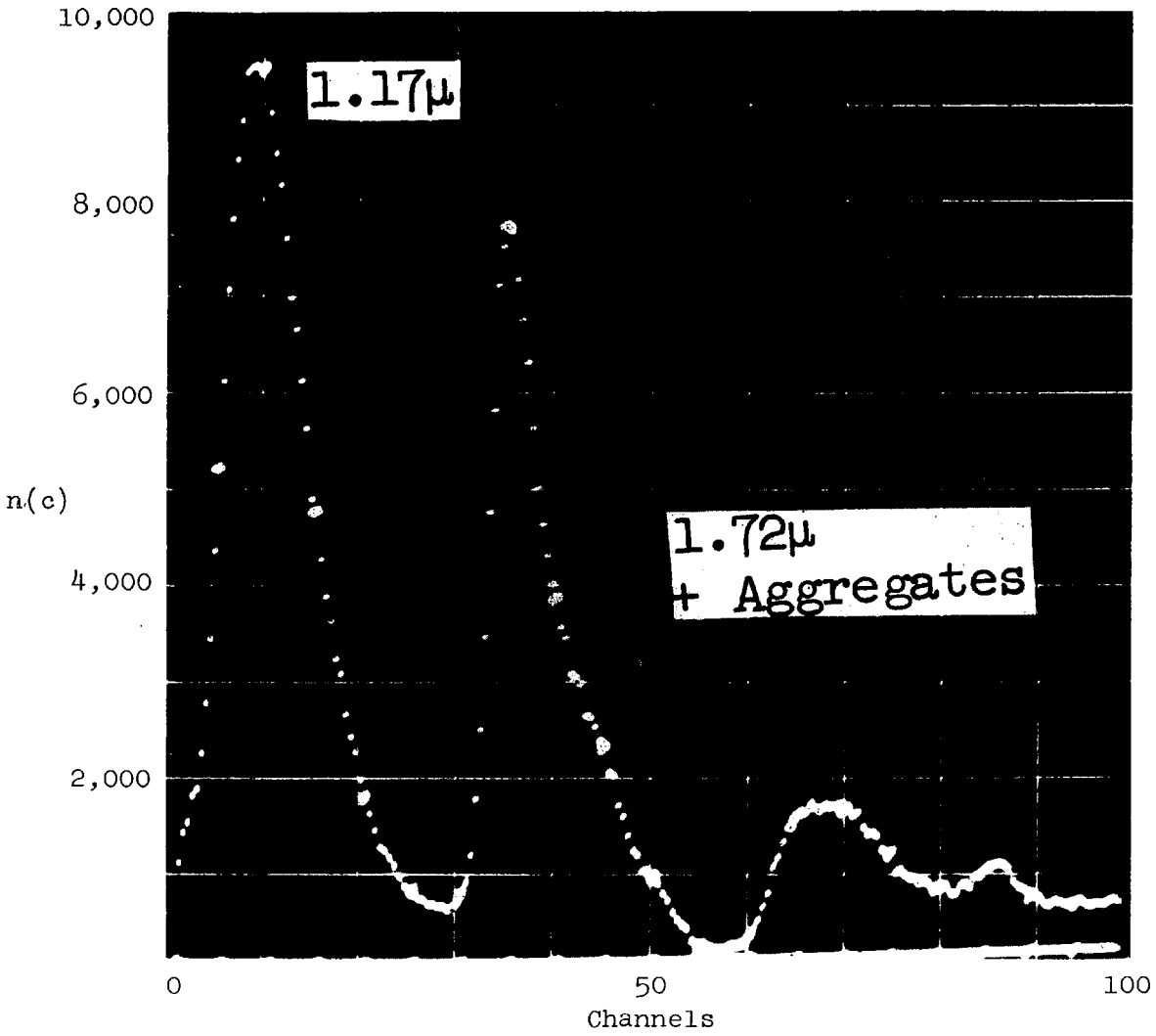

Figure 10. Same distribution as Figure 9, but only the first 100 channels presented.

Figure 11. Analysis of a mixture of 1.17-μ and aggregated 1.72-μ diameter latices. Key: ————————, differential distribution data obtained with multichannel system; ------, data obtained with Coulter counter, model A.

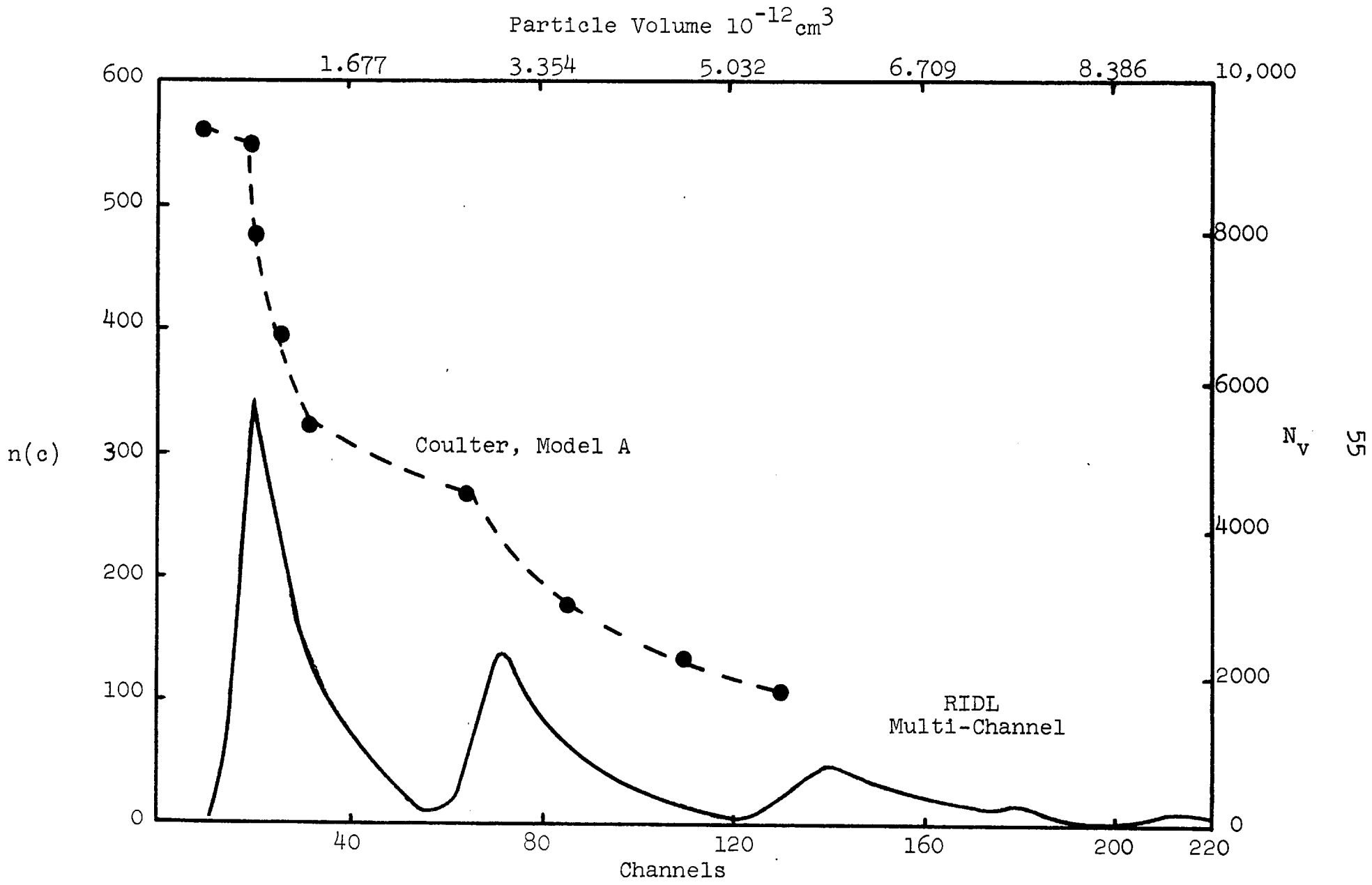
Particle Volume 10^{-12} cm^3
1.677
3.354
5.032
6.709
8.386
10,000
600
500
400
300
200
100
0
n(c)
8000
6000
4000
2000
0
N_v
Coulter, Model A
RIDL
Multi-Channel
40
80
120
160
200
220
Channels

shows the same distribution as in Figure 9 except that the first 100 channels have been expanded by means of the x-axis expansion control. Likewise, the second 100 channels may be expanded for examination of the higher order aggregates.

A quantitative analysis of a mixture of 1.17 and aggregated 1.72-μ latices was carried out with both the multichannel particle analyzer and the Coulter counter, model A, using 30-μ aperture tube. As shown in Figure 11, the multichannel analyzer gives directly a differential distribution, while the Coulter counter gives a cumulative distribution. Whereas the differential data were obtained from one 50-μl. sample, the cumulative distribution was obtained with nine 50-μl. samples. The advantages of the multichannel system can be seen from Figure 11. With the single channel instrument many sample readings must be taken to achieve the same degree of accuracy. For example, if the sixth point in the cumulative plot was not taken, it would have been impossible to decide whether the first two peaks were separate or possibly a single broad distribution. Also, the true particle distribution cannot be adequately resolved for rapid flocculating systems without laborious effort.

To compare the data from the multichannel analyzer with that from the Coulter counter, the differential distributions were integrated planimetrically. Therefore,

$$N_v = \int_v^\infty n(v)dv \qquad \text{(Eq. 32)}$$

where N_v is the integral number of particles larger than v, and n(v)dv is the number of particles between the sizes v and v + dv. The results are tabulated (Table III) and compared with the Coulter counter data.

As the sophistication of the electronics of the multichannel analyzer allows one to detect rapid changes in particle size distributions, the direct display of the differential distributions and the efficient data recording techniques can be utilized with the aid of Eq. 32 to follow the course of aggregation of an initially monosized particle system as a function of time.

Recently, Samyn (56) reported that when suspension systems are highly polydispersed, the Coulter counter, model A, may show poor additive results. This prompted the investigation of the reliability of the multichannel analyzer in this aspect, at least in the range of sizes pertinent to our research. Figure 12 shows (broken curves) the independent distributions of 1.17-μ and aggregated 1.72 and 2.05-μ particles. The noise peak at the 10th channel serves as a reference from which the true particle distribution can be differentiated. Upon mixing equal parts

Figure 12. Distribution curves accounting for additivity in a polydispersed latex system by the RIDL multichannel analyzer. Key: ————, distributions of mixture of equal parts of 1.17, 1.72, and 2.05 μ; —.—.—., independent distribution of 1.17 μ; — — —, independent distribution of 1.72 μ; . . . . ., independent distribution of 2.05 μ.

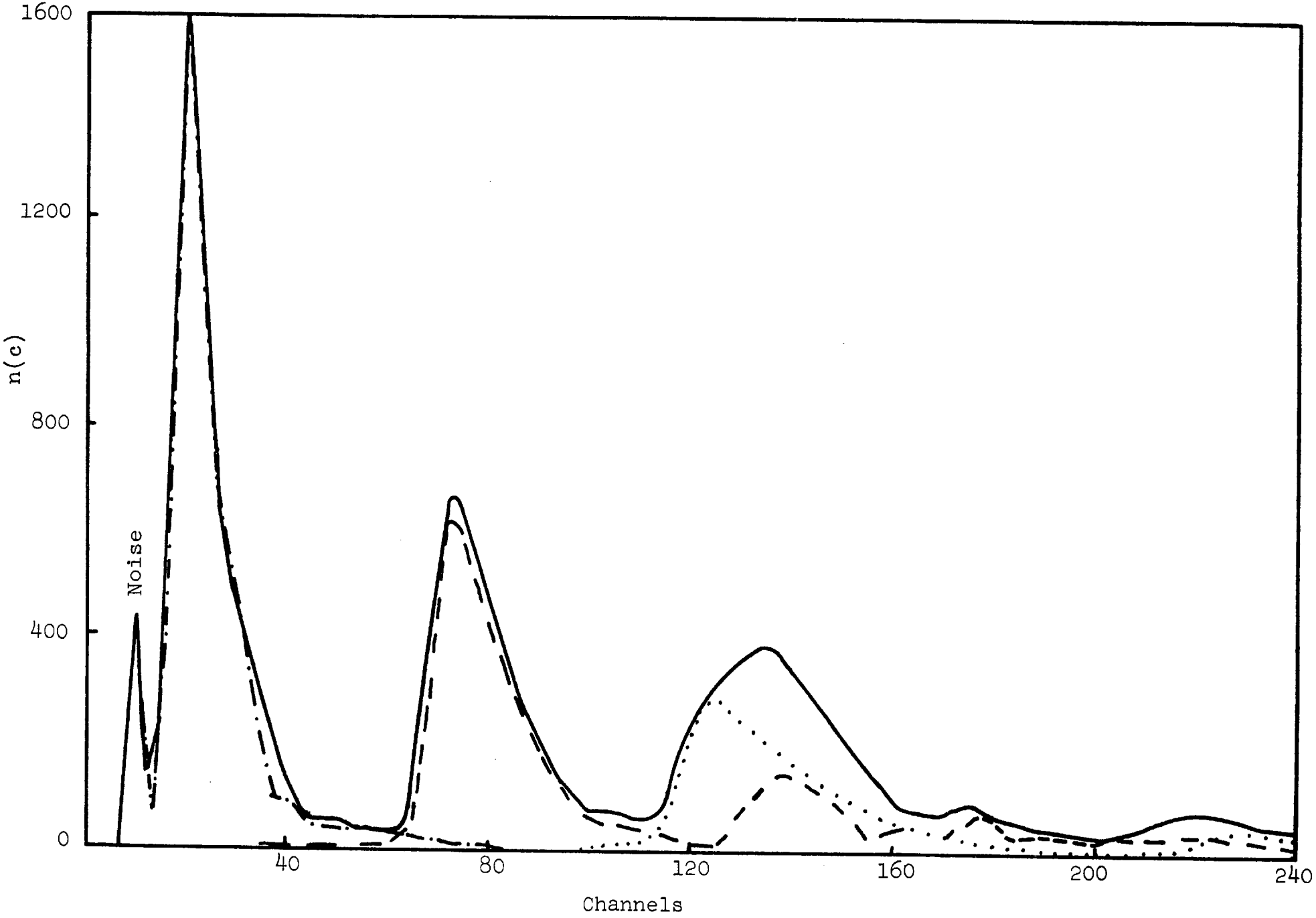
1600
1200
800
400
0
n(c)
Noise
40
80
120
160
200
240
Channels

TABLE III

Comparison of Coulter Counter, Model A, and RIDL Multi-Channel Data on Mixed Latex Particles

Channels	Particle Volume 10^{-12} cm^3	Number of particles beyond stated size	
		RIDL Multi-Channel	Coulter, Model A
10	0.419	9256	9350
20	0.839	8462	8550
40	1.677	5421	5350
60	2.51	4760	4700
80	3.354	3239	3300
100	4.193	2380	2400
120	5.032	1851	1850

of the latex suspensions, the resulting normalized distribution assuming additivity of the separate runs is shown by the smooth curve. It appears therefore that the multichannel analyzer system can give accurate results even when the polydispersity is of the order of thirtyfold in volume.

Because the latex particles are essentially monodisperse, the peak widths given in Figs. 9 through 12 may be used to estimate the instrument resolution. In the present size range this is found to be about $\pm$ 0.1 to 0.2 μ in the diameter. Except in unusual situations, most real suspension systems have broad enough particle size distributions so that the instrument resolution does not constitute a serious limitation.

Results and Discussion

Process of Denaturation

The kinetics and mechanisms of denaturation of ovalbumin by urea are discussed in a number of references (53, 57-61). The initial stage is an intramolecular reaction involving the destruction of internal order. This may be interpreted as the unfolding of the helical structures of ovalbumin to a more randomly coiled arrangement accompanied by an increase in viscosity. Usually, this stage is measured by optical rotation. The second stage is characterized by an increase in viscosity of the solution without further change in optical rotation. In contrast to

the relatively rapid increase in viscosity in the initial stage, the viscosity increases at a slower rate during this second stage and eventually reaches a plateau. It is believed that association of the denatured protein molecules primarily by exchange reaction with sulfhydryl and disulfide groups is an important factor in this second phase. In general, the concentrations of ovalbumin, urea and electrolytes, pH, and temperature all affect this over-all denaturation process.

With the ovalbumin-urea concentration ratios used in this study, the first stage of denaturation is completed within 3 hr. and the viscosity reached a plateau a few hours thereafter.

Flocculation Experiments

Typical differential particle distributions at various time intervals, obtained directly from photographs of the oscillographic display of the multichannel analyzer, are shown in Fig. 13 for the flocculation of denatured protein. In this instance the 30-μ aperture tube was used. Since there was a noise contribution in channels 10 to 13, previously pointed out in Fig. 12, only that portion of the distribution from the 15th channel was used for further analysis.

Figure 14 gives the cumulative counts versus time curves showing flocculation of denatured ovalbumin at times greater than about 60 minutes. These results were planimetrically determined from data

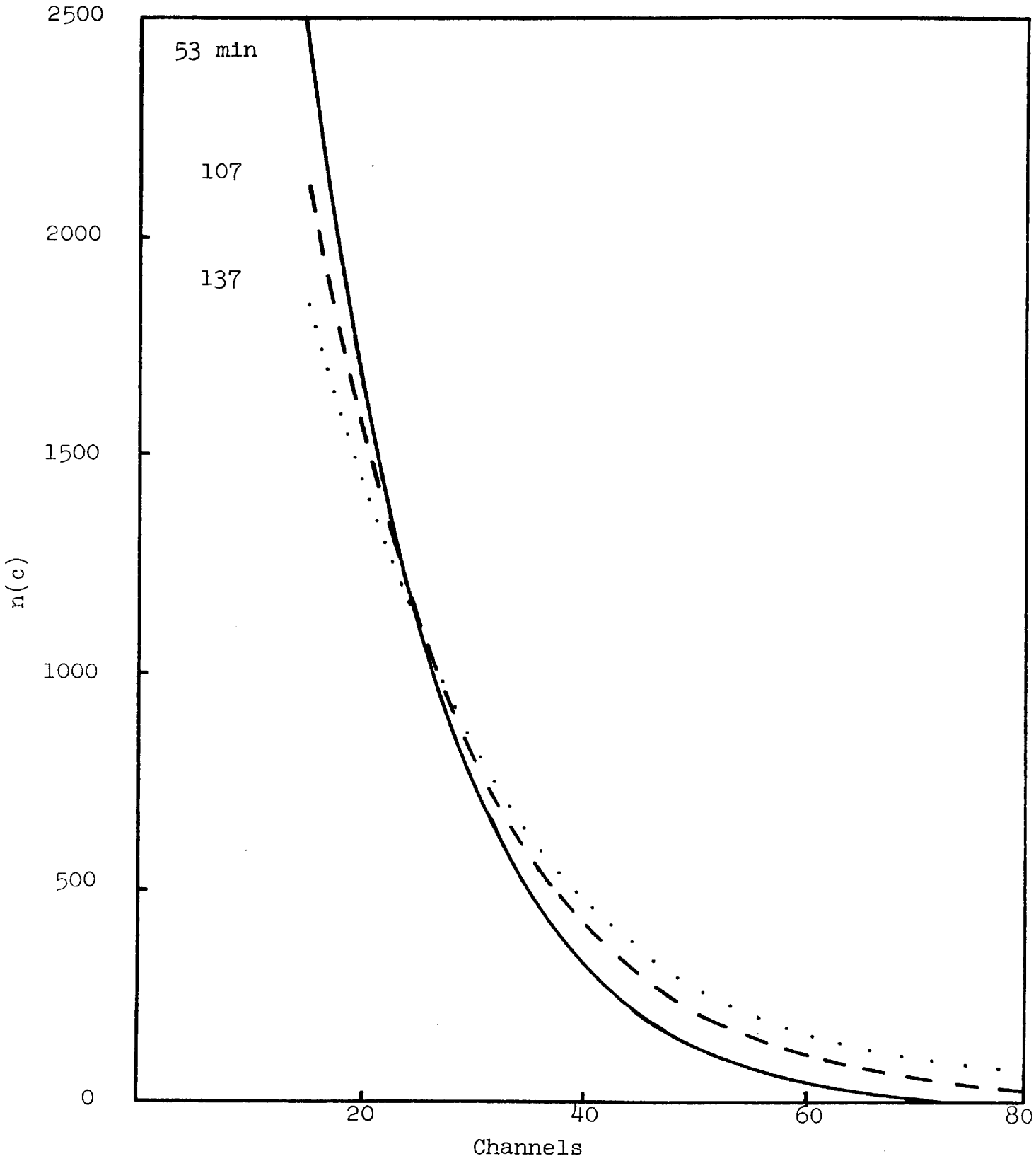

Figure 13. Differential distribution data showing flocculation of denatured ovalbumin particles with time in buffered saline, pH = 4.6.

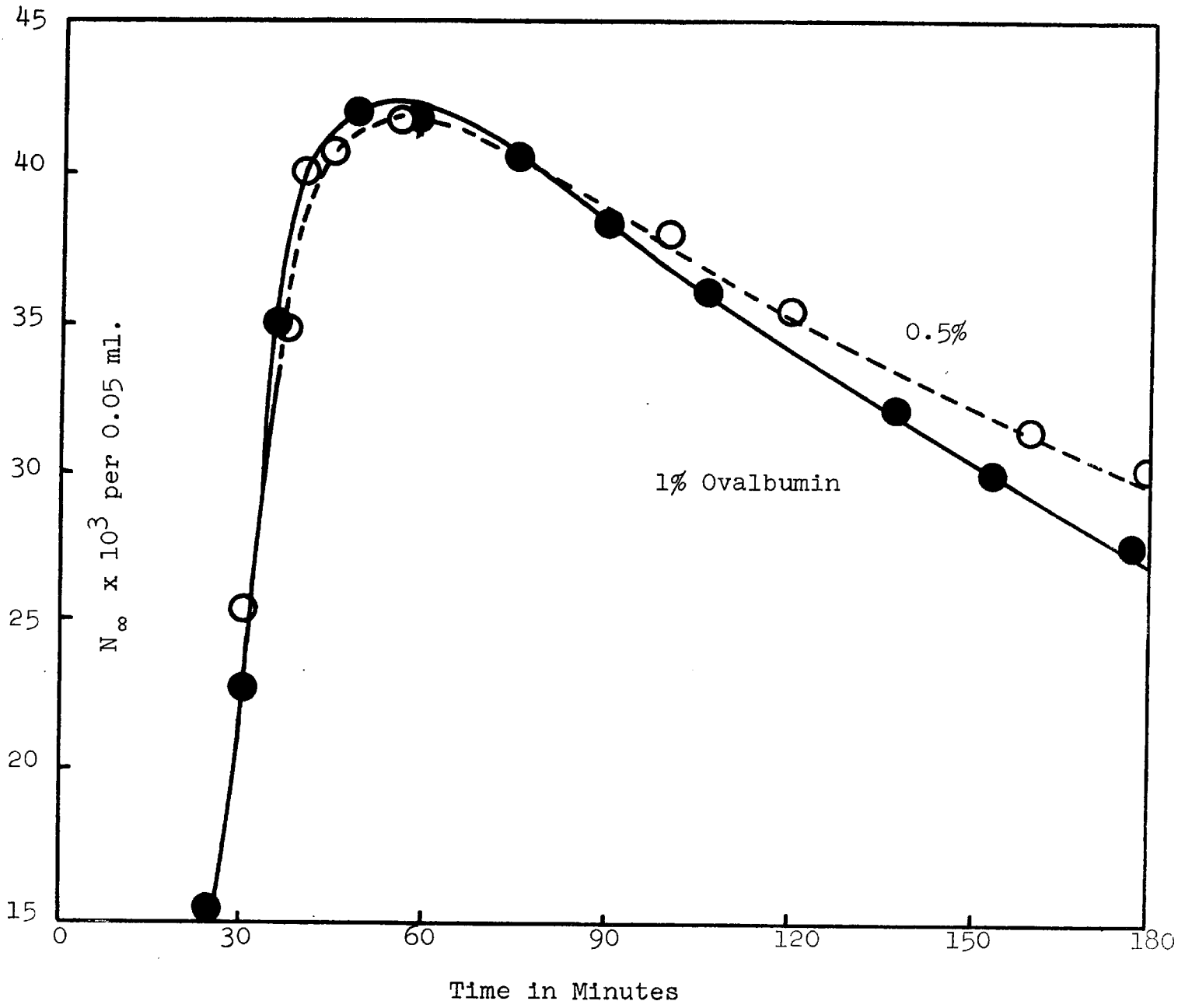

Figure 14. Changes in total denatured protein particulate concentration for sizes greater than 0.80-μ diameter as a function of time. Decreasing counts after 60 min. reflect flocculation of particles.

such as those given in Fig. 13. The pH is in the neighborhood of the isoelectric point for denatured ovalbumin. The two curves correspond to the 0.5% and the 1.0% protein denatured for 24 and 22 hr., respectively. For longer denaturation times the results were essentially the same.

Mass balance was approximately maintained after times greater than the time corresponding to the peak shown in Fig. 14. This was established by graphical integration,

$$M = \int_{v}^{\infty} \rho v n(v) dv \qquad \text{(Eq. 33)}$$

where M is the protein mass, ρ is the density, v is the volume of the particle, and n(v)dv is the number of particles between the sizes v and v + dv.

The range of sizes observed in these experiments was 0.4 to 1.2-μ radius. The majority of the particles were between 0.4 to 0.8-μ radius. Under the microscope, X970 in immersion oil, the flocs were found to be nearly spherical in shape and were in the general magnitude of sizes detected by the multichannel analyzer.

Comparison with Smoluchowski's Theory

By using Eq. 32 the changes of the cumulative number of particles, N_∞ , with time were determined by graphical integration with a planimeter of such differential particle distribution data, as shown in Fig. 13. In the present experiments N_∞ corresponds to the total number of particles larger than the particle volume of 0.6289×10^{-12} cm.^{3} (15th channel),

although the distribution extended to smaller sizes. The Coulter counter, model A, gave this quantity directly by using the appropriate threshold setting. In Fig. 15, the straight line relationship of the Smoluchowski-type plot is found. This is consistent with the theory of flocculation of essentially monodispersed sols. The experimental rate constants obtained with the 30 and 50-μ aperture tubes were not significantly different. The data much beyond 200 minutes were believed to be unreliable because of the effects of sedimentation upon the aggregation rate. According to Müller (62), at room temperature, sedimentation may significantly affect the rate constant when the radius of some of the denatured ovalbumin particles is larger than 2 to 3μ.

In Table IV the summary of some flocculation experiments of urea-denatured ovalbumin is given. The rate constant obtained from the multichannel analyzer and the Coulter counter compared well with each other and also with theory. Once the denatured protein solution reached a constant viscosity level, subsequent rate constants found did not differ from each other. There is a strong dependence of pH on the flocculation. Maximum flocculation was found near the isoelectric point. At pH 5.5 insignificant counts were detected with the 30-μ aperture tube. However, the Tyndall beam showed the presence of many submicron particles in a sol that remained stable for at least 4 weeks. At higher pH values, the Tyndall was weaker.

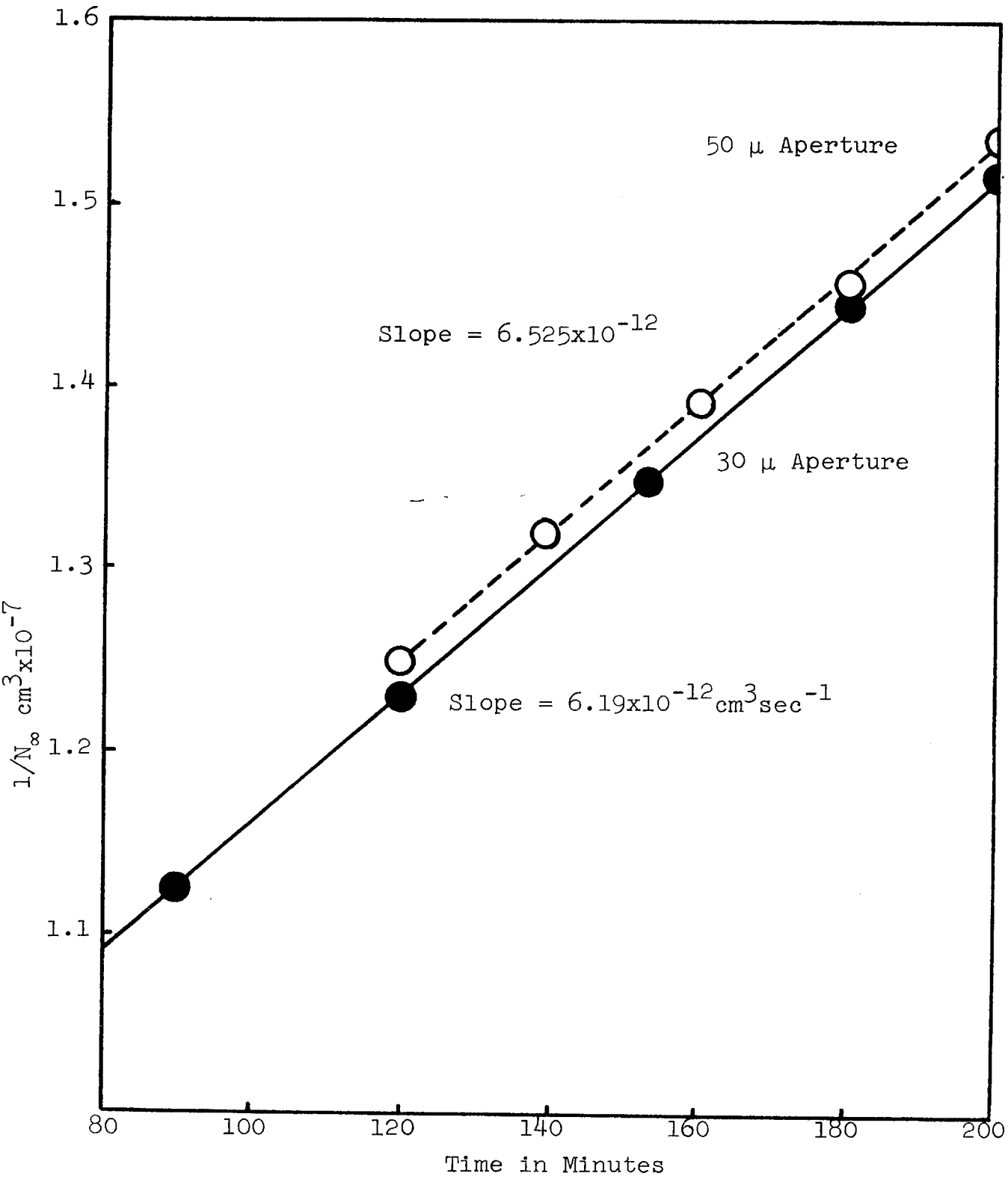

Figure 15. Linear plots showing agreement of the flocculation time data with Smoluchowski theory.

TABLE IV

Summary of Data on Flocculation of Urea-Denatured Ovalbumin

% Protein Concentration	pH Buffered Normal Saline	Denaturation Period (Hrs.)	$K_s \times 10^{-12}$ (cm.^{3}sec.$^{-1}$)	
			Coulter, Model A	RIDL Multi-Channel
0.5	4.6	24	5.62	6.43
		64	5.90	6.19
	5.5	64	Insignificant counts, but weak Tyndall beam observed.	
	8.7	64		
1.0	4.6	22	----	7.23
		49	7.1	7.67
	5.5	49	Insignificant counts, but weak Tyndall beam observed.	
	8.7	49		

Comparison with the Self-Preserving Theory

The theory was applied to the denatured protein system for the data partially shown in Fig. 13. A log-log plot of N_v versus v is shown in Fig. 16 and values of N_∞ were determined by extrapolation of the curve to small values of v. When a Smoluchowski-type plot was made using the extrapolated values, the rate constant was 5.91×10^{-12} cm.^{3} sec.$^{-1}$ previously found by using that part of the data at larger sizes. The volume fraction was 3.56×10^{-8} cm.^{3} for 0.05-ml. sample of the sol in contrast to the theoretical 3.58×10^{-8} cm.^{3} to indicate that after 53 minutes practically all of the insoluble protein came into the detectable range of the RIDL analyzer system. In Fig. 17 the plots of N_v/N_∞ versus η at different time intervals shows the tendency of the distribution to preserve its form and gives ψ_2, the time-independent dimensions cumulative distribution function, as predicted by Eq. 16.

According to the theory, the effect of the heterogeneity of the particle size distribution (A_1) and the collision efficiency ($\alpha = 1/W$) on the flocculation rate constant can be determined. By using the data in Fig. 17 and graphical integration of the appropriate values of η versus ψ_2 plot as indicated by Eq. 18, A_1 was found to be 4.148 ± 0.022. This value A_1, compared to a value of 4.0 for homogeneous flocculation, indicates that heterogeneity resulted in about a 4 per cent increase in rate. Assuming that the floc-

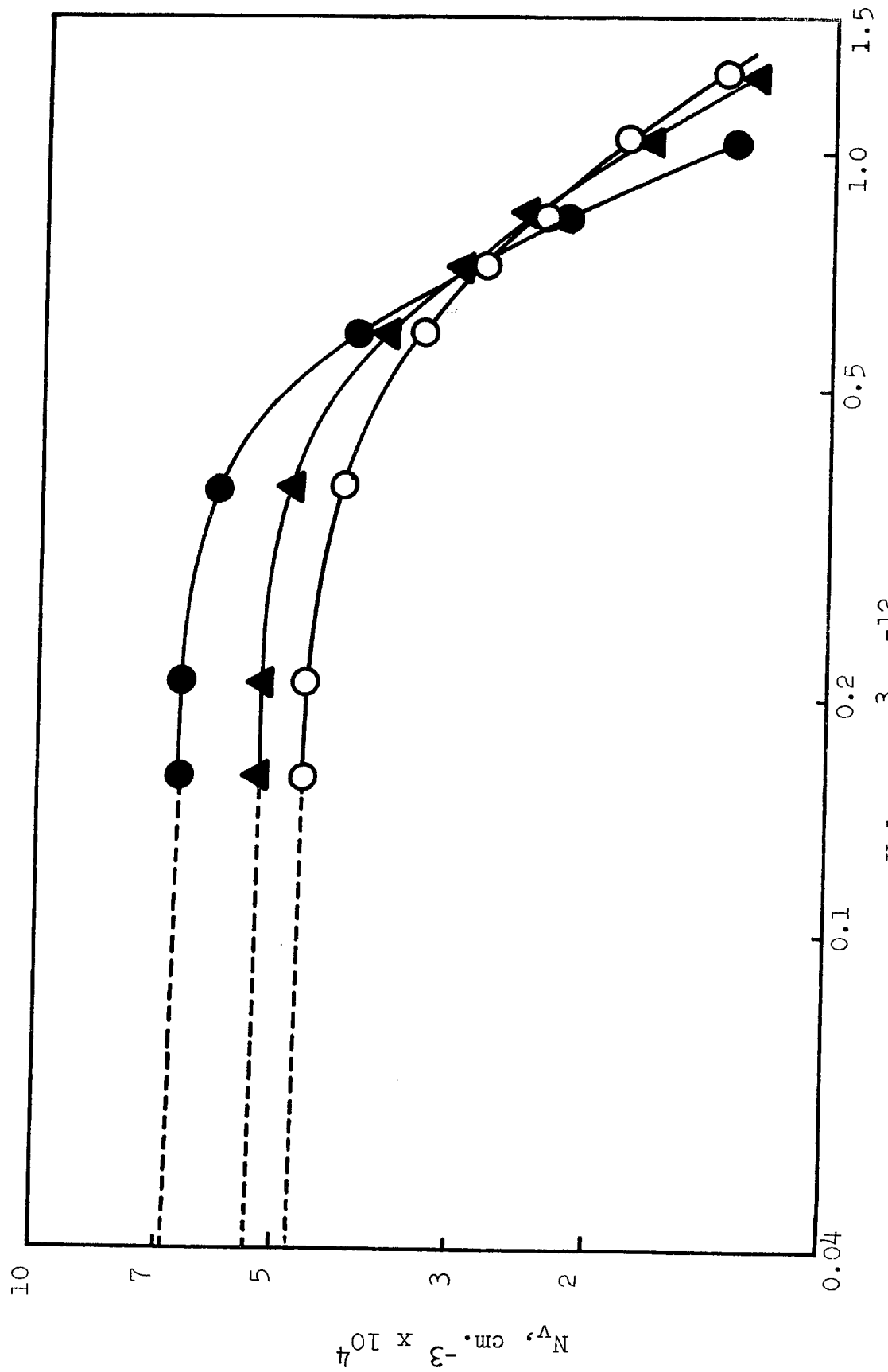

Figure 16. Cumulative size distributions for flocculating denatured ovalbumin particles. Key: ●, 53 min.; ◀, 107 min.; ○, 137 min.

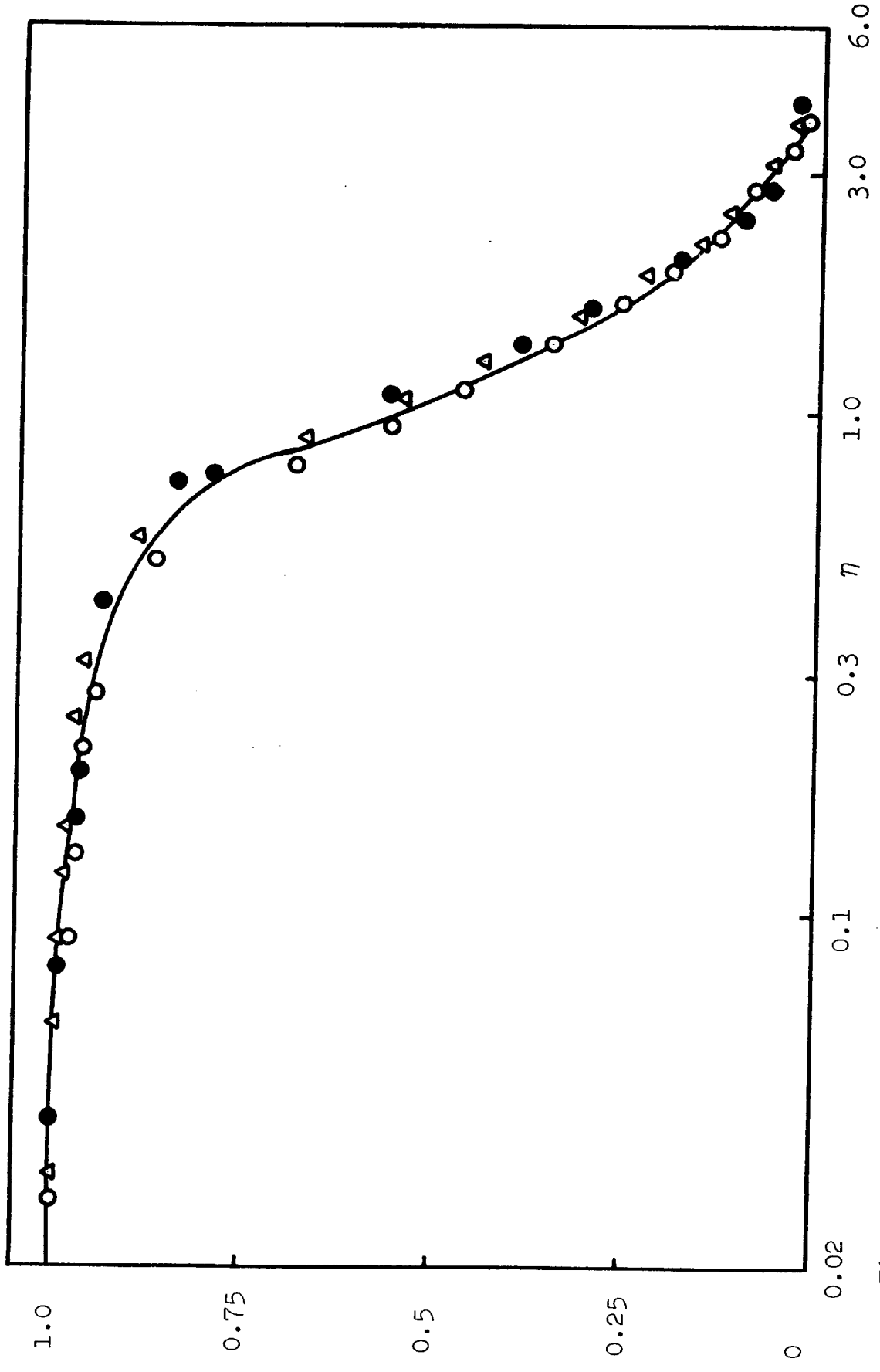

Figure 17. Test of self-preservation theory for flocculating denatured ovalbumin particles. In terms of dimensionless distribution functions, particle distributions taken at different times during the flocculation process fall approximately on a single curve. Data taken from Figure 16.

TABLE V

Comparison of Methods of Determining
Rate Constants of Flocculation

Method of Treatment	$K_s \times 10^{-12}$ ($cm.^3 sec.^{-1}$)
Smoluchowski's theory for monodispersed distribution taking N_∞ from	
(a) $\geq v = 0.6289 \times 10^{-12} cm.^3$	6.19
(b) $\geq v = 0.02 \times 10^{-12} cm.^3$	5.91
Self-preservation theory	5.81

culation is rapid so that $\alpha = 1$, the rate constant calculated by the self-preservation theory was 5.81×10^{-12} cm.^{3} sec.$^{-1}$ If the values of $K_s = 5.91 \times 10^{-12}$ and A_1 are substituted in Eq. 18, the collision efficiency α is found to be 1.03 and, correspondingly, the Fuch's stability factor W is nearly unity. The comparison of methods of determining the rate constant is summarized in Table V. It should be noted that the approach of self-preservation theory offers a method of determining the flocculation rate constant independent of that approach which assumed a monodispersed system at initial periods of the flocculation process. Since the effective collision between particles was unity and the particle size distribution was essentially monodispersed, the rate constants determined by both methods were in good agreement.

SECTION IV

QUANTITATIVE STUDIES OF PARTICULATE MATTER IN PARENTERAL SOLUTIONS

This is an exploratory study of the problem of particulate matter in parenteral solutions. It emphasizes the methodology of sizing and counting particles and the physical significance of the particle size distributions found.

Experimental

Materials

Large volume, sterile intravenous solutions from a pharmaceutical manufacturer and a hospital pharmacy were used. These included 10 samples each of one liter size solutions of normal saline and dextrose 5% in 0.2% sodium chloride solution from single lots. The container system used by the pharmaceutical manufacturer differed from that by the hospital pharmacy in that the former is a screw-capped container and the latter is a hermetically, vacuum-sealed container with a rubber closure-air vent tube system. Also, six multiple-dose vials of penicillin G potassium (20 million units) and chloramphenicol sodium succinate (1.0 gm.) were used, both representing a classification of injections containing sterile solids which yield a solution upon

reconstitution with a diluent.

Determination of the Particle Size Distribution

Cumulative particle size distributions of the injection samples were determined with the Coulter counter,[7] model A, and a 50 μ aperture tube. Various precautions were taken to avoid possible accidental particle contamination. As shown in Fig. 18, the bulk IV solution is introduced to a sample tube, enclosing the aperture system of the particle counter, with an IV solution administration set[8]. In this closed manner, the administration set and sample tube may be repeatedly filled and flushed. Since the conductivity of the solution between the aperture must be the same, a solution containing the same electrolyte concentration as in the sample is introduced into the inner compartment of the aperture tube from an outside source. To accommodate the screw-cap type container, a special plastic adapter cap[9] for the administration set was used. This particular sampling setup is also adaptable for the determination of particle contamination in various solution administration and transfusion assemblies, syringes and needles, using normal saline solution in which the particle size distribution has been already determined.

---

[7] See Section III, p. 47 for the calibration.

[8] Plexitron R-41 by Baxter Laboratories, Inc., Morton Grove, Illinois.

[9] BA-3 adapter cap by Baxter Laboratories, Inc., Morton Grove, Illinois.

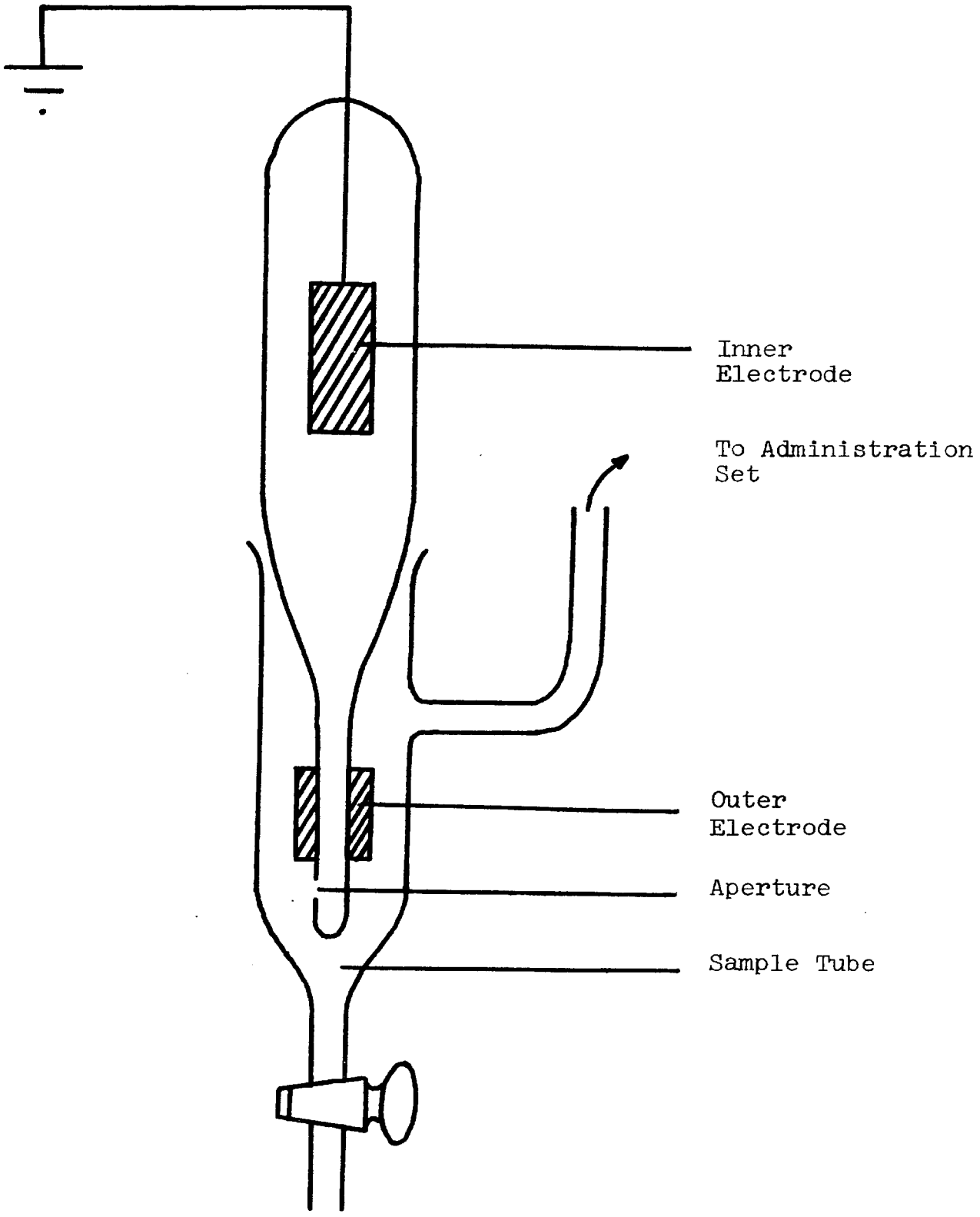

Figure 18. Sampling chamber for the Coulter counter used for the determination of particle size distributions in parenteral solutions.

To count and size particles with the Coulter counter for non-electrolyte parenteral preparations, such as dextrose, mannitol, and lyophillized drugs, a sufficient quantity of electrolyte must be added. The reconstitution of the penicillin and chloramphenicol injections was performed in the following manner. After removing the rubber closure from the vial, normal saline, previously standardized with the particle counter was added with a pre-flushed syringe and needle. The procedure was carried out in an aseptic, positive pressure room. With a syringe and needle, the reconstituted solution was transferred to the sample counting chamber (Fig. 18).

For accurate counting at various threshold sizes, particularly for low particle concentrations, the sample volume flowing through the aperture was pre-set for at least 0.5 ml. All determinations were made in duplicate. No specific attempt was made to identify the particles, except by visual examination.

Results and Discussion

The cumulative particle size distribution for the normal saline solutions are shown in Fig. 19 and are compared with the proposed Australian standard. The normal saline from the pharmaceutical manufacturer was "cleaner" than those made by the hospital pharmacy by approximately a factor of 2 and differed from the Australian standard by a factor of 6. Although the particle distributions of dextrose 5% in 0.2% NaCl solutions of both manufacturers are not shown, they were

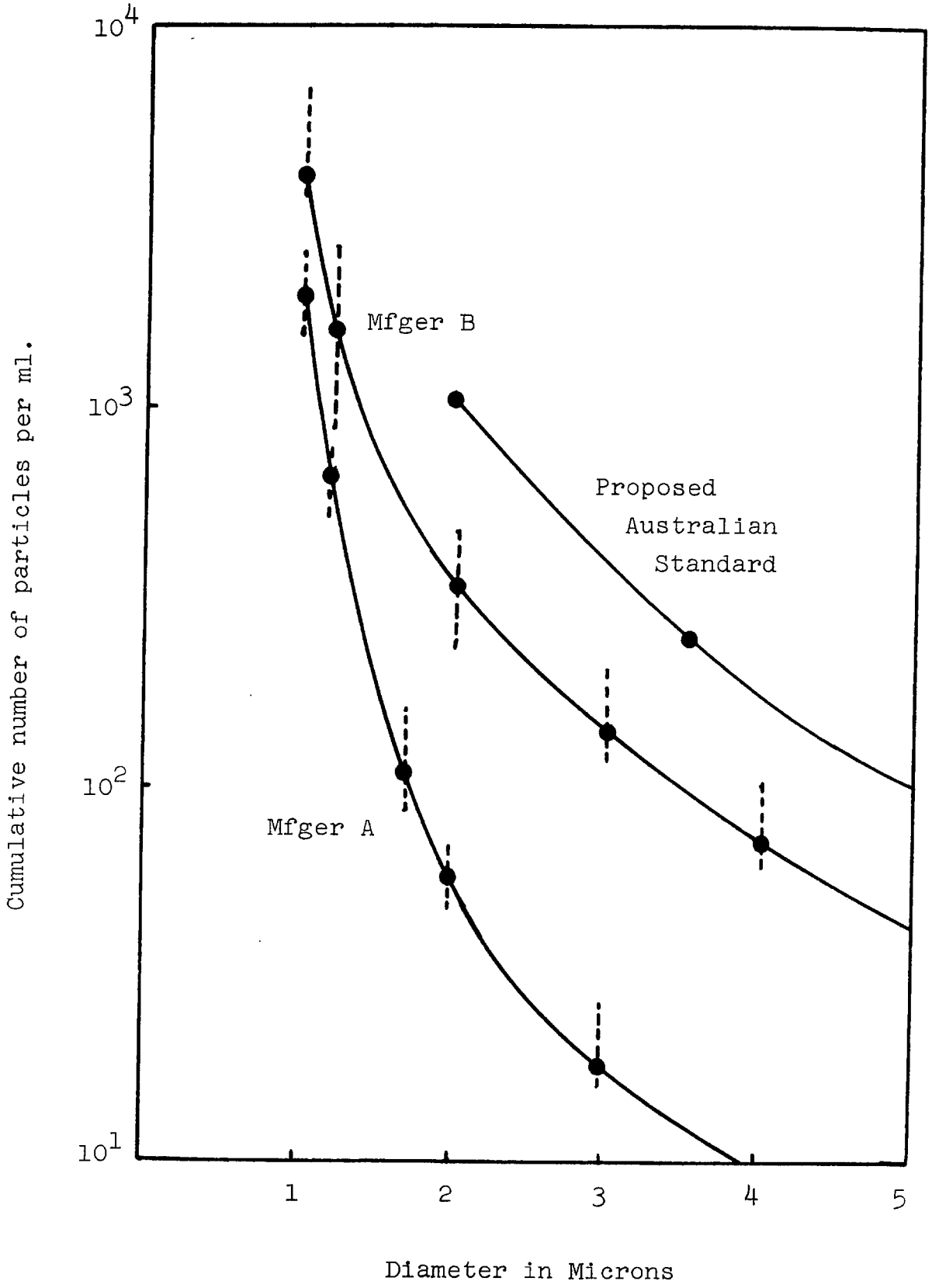

Figure 19. Cumulative Particle Size Distributions in Normal Saline for Injection in One Liter Containers.

within those distributions found in the worst and best normal saline bottles of the respective manufacturers. However, the results show that large volume intravenous solutions can meet a standard of clarity, such as that defined in Australia, with the present state of technology and manufacturing quality control practices.

In Fig. 20 the cumulative particle distribution per injection container of penicillin and chloramphenicol, corrected for the background distribution of the normal saline diluent, is shown. The plot represents average counts with a range of $\pm$ 5 per cent. Visual examinations revealed the predominating presence of fibers and sometimes a few glass and rubber pieces.

Since the accurate sizing and counting are interrelated and are important criteria for the disposition of any parenteral solution, the limitation of any electronic particle counter should be recognized (63). For example, the performance of the Coulter counter will be affected by such physical parameters as the size of the particle relative to the size of the aperture, shape, surface roughness, conductivity of the particle and orientation of the particle in the aperture. While it is the particle volume, relative to a non-conducting latex sphere standard, that is determined, the diameter is calculated on the basis of an equivalent sphere. Then the use of this dimension is a naive way of describing a non-spherical particle, for example, a relatively long cylinder like a cotton fiber.

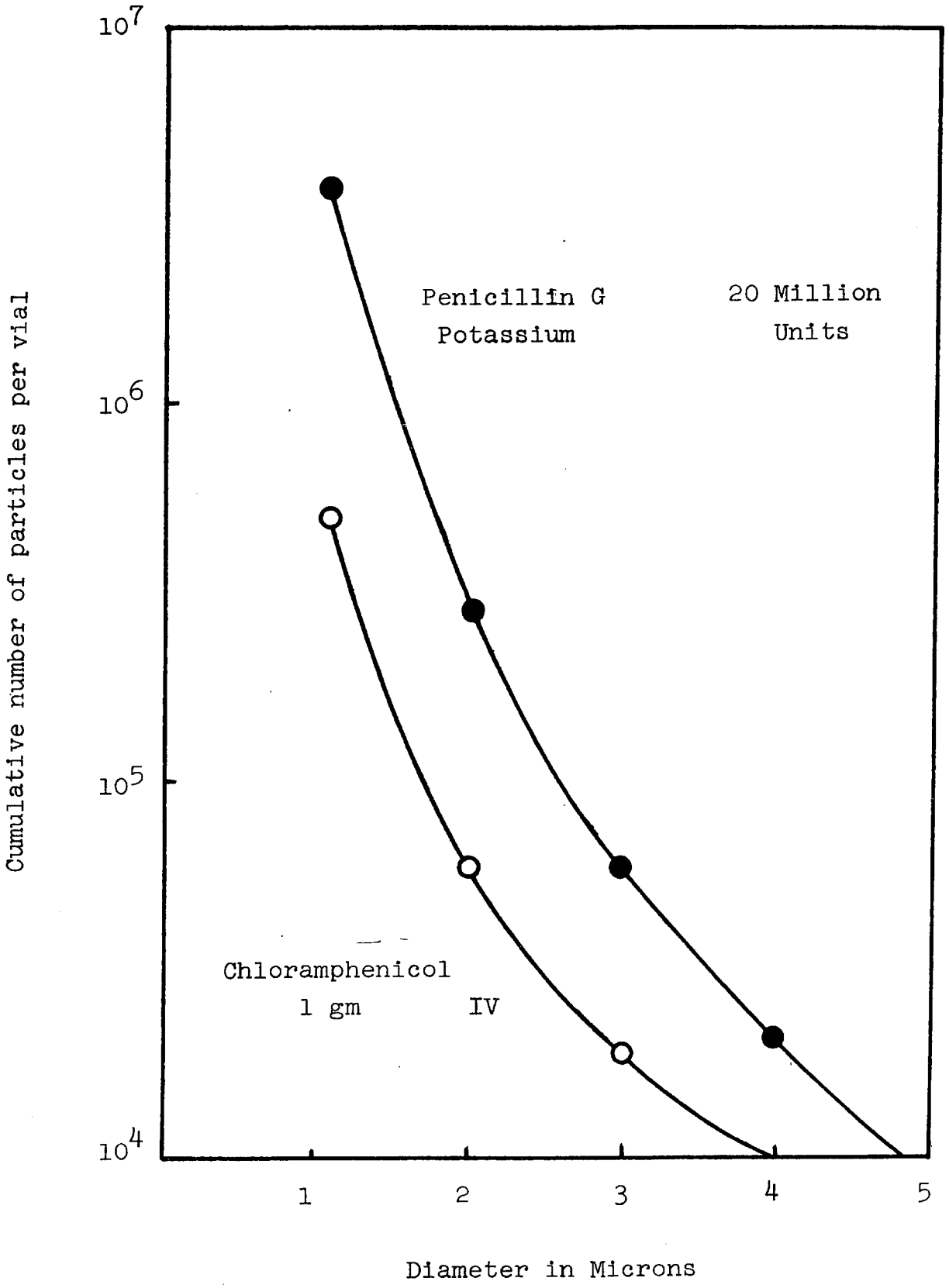

Figure 20. Cumulative Particle Size Distributions in Vials Containing Penicillin G Potassium and Chloramphenicol Sodium Succinate.

In the final analysis, the size distribution and composition of the particle which is delivered into the patient's circulatory system are the important things of great concern. Therefore, the efforts of a manufacturer to produce high quality solutions are defeated when the solution becomes contaminated by dirty solutions, administration sets, syringes and needles, coring of rubber stoppers, faulty techniques at the patient's bedside, drug additive and airborne particles. Very little is known about the quality of solutions relative to shelf-life conditions. Constituents in rubber closures and plastic formulations or their reaction products are known to leach out and provide potential sources of particulate matter (64). Flocculation may change the particle distribution with time. Although there are many variables influencing flocculation in practical situations during the actual storage and handling of parenteral solutions while enroute to distribution centers and hospitals and while within hospitals, let us hypothetically attempt to approximate the degree of flocculation of the worst container of normal saline, which particle concentration was found to be 7000 per $cm^3 \geq 1 \mu$ diameter. Assuming that (a) no additional particles are entering into the system from the container components, (b) there are no particles less than 1μ and (c) flocculation occurs according to Smoluchowski's rapid flocculation theory for a non-sedimenting and non-turbulent monodispersed system

at room temperature, a half-life of 334 days is predicted. In any respects, this suggests the probable need for some expiration date based not only on chemical stability but also on the changing distribution of particle sizes with time.

Perhaps, the findings of the exploratory study can be summarized by considering a typical prescription for the treatment of spinal meningitis by the intravenous route. The prescription for penicillin and chloramphenicol in dextrose 5% with 0.2% NaCl and the total particle concentrations for each drug, extrapolated from the data in Figs. 19 and 20, is shown in Table VI. At least 1.2×10^7 particles $\geq 1\,\mu$ diameter would be potentially introduced into the patient's vein. Furthermore, a patient of this type may receive as much as two liters daily for 3 to 4 days. If so, at least 7.2×10^7 particles will be needlessly included as part of the drug therapy.

TABLE VI

Possible Cumulative Number of Particles
in a Typical Intravenous Solution Prescription

Prescription	Number of Particles $\geq 1\ \mu$ Diameter
Penicillin G Potassium, 20 million units	3.79×10^6
Chloramphenicol Sodium Succinate, 2.0 gm.	1.02×10^6
Dextrose 5% in 0.2% NaCl One Liter	7.1×10^6
Total number of Particles $\geq 1\ \mu$	11.91×10^6

SUMMARY AND CONCLUSIONS

This thesis has described the development of quantitative methods as well as the development and application of theoretical considerations so that studies involving particle-particle interactions in certain biopharmaceutical, clinical biochemical and biologic systems can be handled.

A theoretical study of preferential coalescence and aggregation of small particles in herterodispersed systems was carried out where moderate electrical barriers exist between the particles. Equations based on the concepts of Derjaguin, Verwey, and Overbeek were employed. Computations over a wide range of conditions have shown that small particles may aggregate (or coalesce) with themselves or with larger particles at rates that are ten to fifty orders of magnitude faster than particles ten times larger. These findings may explain (a) the relatively narrow particle size distributions observed in certain emulsions and flocculated suspensions and (b) the limited flocculation and coalescence behavior observed in certain instances.

A method of studying the kinetic and mechanism of flocculation of denatured protein particles was

developed, using a procedure based on the RIDL multi-channel particle counter and size analyzer system. The precipitation behavior of urea denatured ovalbumin in normal saline was studied near its isoelectric point. An evaluation of the data showed that the Smoluchowski theory for rapid flocculation of monodispersed particles and the self-preservation theory satisfactorily accounted for the results. The flocculation appeared to involve the formation of relatively uniform primary particles of around one micron diameter. Such narrow distributions are consistent with the limited flocculation theory that selective flocculation of small particles with large ones takes place. At pH 5.5 and above, the particle sizes were smaller than 1 μ and the colloidal system remained stable for at least 4 weeks. Among other areas of study, the results indicate that further research effort should be directed to a specific area, that is, reversible flocculation due to pH changes, protein solubility, solvation layer and electrostatic effects.

The problem of particulate matter in parenteral solutions was explored. The particle size distribution in some large volume intravenous solutions and lyophillized injections was quantitated using the Coulter counter and a special sampling chamber. The results showed that the samples of the large volume parenteral solutions met the proposed Australian standard of clarity.

APPENDIX I

Attractive Potential Energy between Unequal Spheres and the Effect of Retardation

Hamaker (10) was the first to describe the potential energy of attraction between unequal spheres, $V_{A(S_1/S_2)}$, of similar constitution. For a_1, $a_2 >> H$, the limiting expression is

$$V_{A(S_1/S_2)} = -\frac{Aa_1a_2}{6(a_1 + a_2)H} \qquad \text{(Eq. I-1)}$$

where Hamaker's constant $A = \pi^2 q^2 \beta$, and q is the number of atoms per cm^3, β is the London constant, a_1, a_2 and H are defined as before. The evaluation of Hamaker's constant is also discussed elsewhere (65, 66).

Schenkel and Kitchener (49) made a thorough analysis of the retardation effect. Using the equations for f(p) as a check that are presented in several references (42, 67), they derived empirical expressions that gave the best fit and that would give an analytic solution for interaction energies with modifications for the retardation effect. Accordingly, for the range of $0.5 < p < \infty$,

$$f(p) \sim \frac{2.45}{p} - \frac{2.17}{p^2} + \frac{0.59}{p^3} \qquad \text{(Eq. I-2)}$$

For comparatively large distances, Casmir and Polder (68) showed that the London energy between atoms

decay very rapidly due to retardation effects. Consequently, the London interaction energy of a pair of atoms of r distance apart,

$$V_{A(London)} = -\frac{\beta}{r^6} \qquad \text{(Eq. I-3)}$$

must be corrected so that

$$V'_{A(at./at.)} = V_{A(London)} f(p) \qquad \text{(Eq. I-4)}$$

where $p = 2\pi r/\lambda$ and λ is the characteristic wavelength of the atoms and β is the London constant. Equation I-4 may be rewritten

$$V'_{A(at./at.)} = -\frac{2.45\lambda\beta}{2\pi r^7} + \frac{2.17\lambda^2\beta}{(2\pi)^2 r^8} - \frac{0.59\lambda^3\beta}{(2\pi)^3 r^9} \qquad \text{(Eq. I-5)}$$

In deriving the expressions for the retarded interaction energies for equal spheres, Schenkel and Kitchener used Derjaguin's method (69, 70) for calculating the interaction of spheres. It was pointed out that the algebra was simpler than for Hamaker's method (10) and that the results obtained were the same by both methods, provided it is only the limiting expressions that are required. In a likewise manner, the method is applied to the interaction between unequal spheres.

Applying equation I-4 to the geometry in Fig. 21, the interaction energy between an atom and all of the atoms in an infinitely large flat plate, $V'_{A(at./p)}$, may be described by the superposition of their retarded attractive energies, i.e.

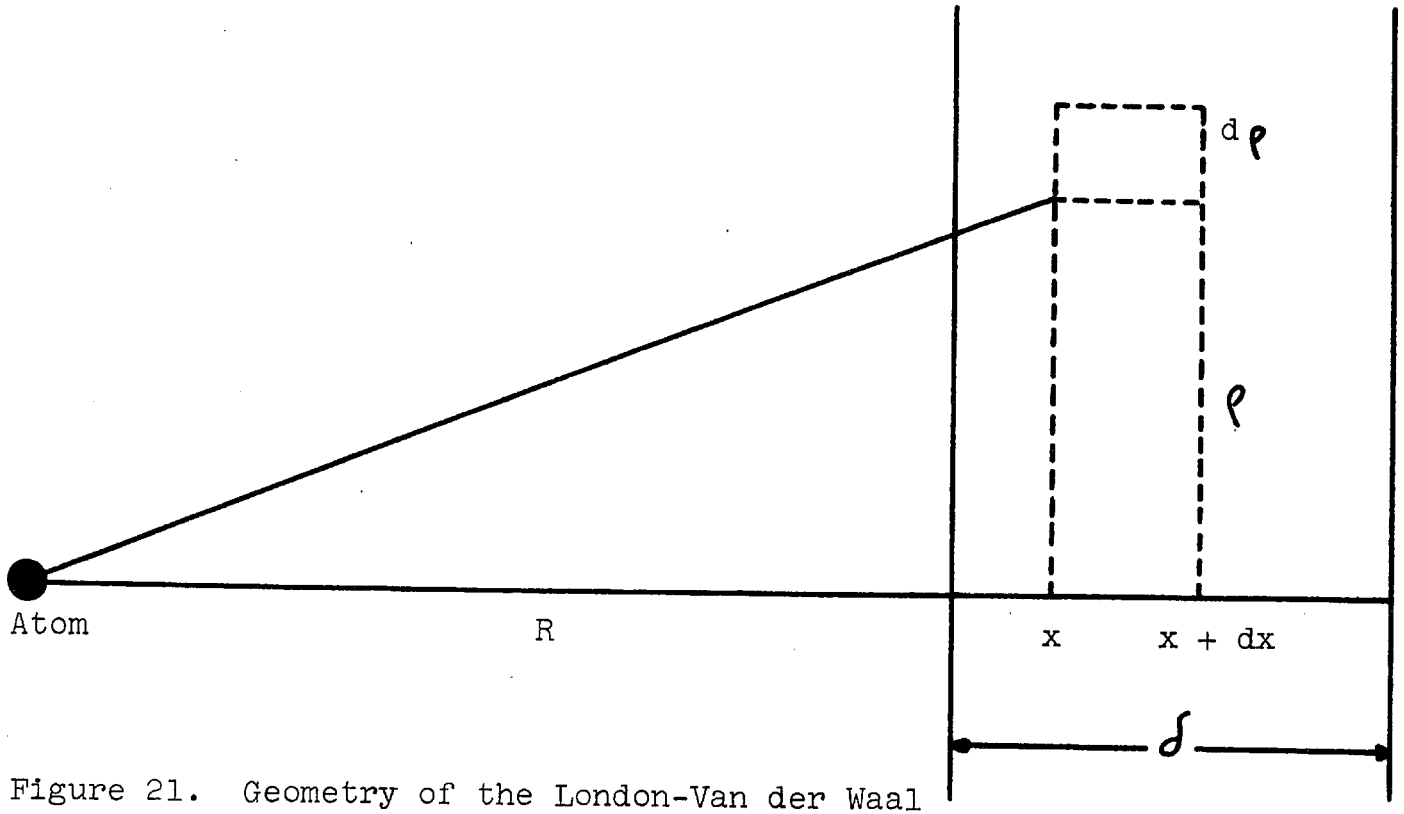

Figure 21. Geometry of the London-Van der Waal interaction between an atom and an infinitely large plate of thickness δ. The plate is built up of infinitesimal small rings of diameter ρ, cross-section $d\rho\, dx$ at a distance $(R + x)$ from the atom (71).

$$V'_{A(at./p)} = V''_A + V'''_A + V''''_A \qquad \text{(Eq. I-6)}$$

where

$$V''_A = -\int_o^{\delta}\int_o^{\infty} \frac{2\pi q \phi \rho \, d\rho \, dx}{[(R+X)^2 + \rho^2]^{7/2}} \qquad \text{(Eq. I-7)}$$

$$V'''_A = \int_o^{\delta}\int_o^{\infty} \frac{2\pi q \theta \rho \, d\rho \, dx}{[(R+X)^2 + \rho^2]^{4}} \qquad \text{(Eq. I-8)}$$

$$V''''_A = -\int_o^{\delta}\int_o^{\infty} \frac{2\pi q Z \rho \, d\rho \, dx}{[(R+X)^2 + \rho^2]^{9/2}} \qquad \text{(Eq. I-9)}$$

and $\phi = \frac{2.45\lambda\beta}{2\pi}$; $\theta = \frac{2.17\lambda^2\beta}{(2\pi)^2}$; and $Z = \frac{0.59\lambda^3\beta}{(2\pi)^3}$. Also, the Hamaker constant $A = \pi^2 q^2 \beta$. It follows that the interaction between two flat plates, $V'_{A(p/p)}$ is

$$V'_{A(p/p)} = \int_R^{\infty} q \, V'_{A(at./p)} \, dR \qquad \text{(Eq. I-10)}$$

If the surface of two spheres is thought to be built up of parallel pairs of infinitesimally small rings with radius h, the interaction of unequal spheres, $V'_{A(S_1/S_2)}$, is expressed by

$$V'_{A(S_1/S_2)} = \int_o^{\infty} 2\pi V'_{A(p/p)} h \, dh \qquad \text{(Eq. I-11)}$$

From the geometry in Fig. 22,

$$H - H_o = a_1 + a_2 - \sqrt{a_1^2 - h^2} - \sqrt{a_2^2 - h^2} \qquad \text{(Eq. I-12)}$$

After differentiating and noting that $a_1, a_2 \gg h$,

$$h\,dh \simeq \left(\frac{a_1 a_2}{a_1 + a_2}\right) dH \qquad \text{(Eq. I-13)}$$

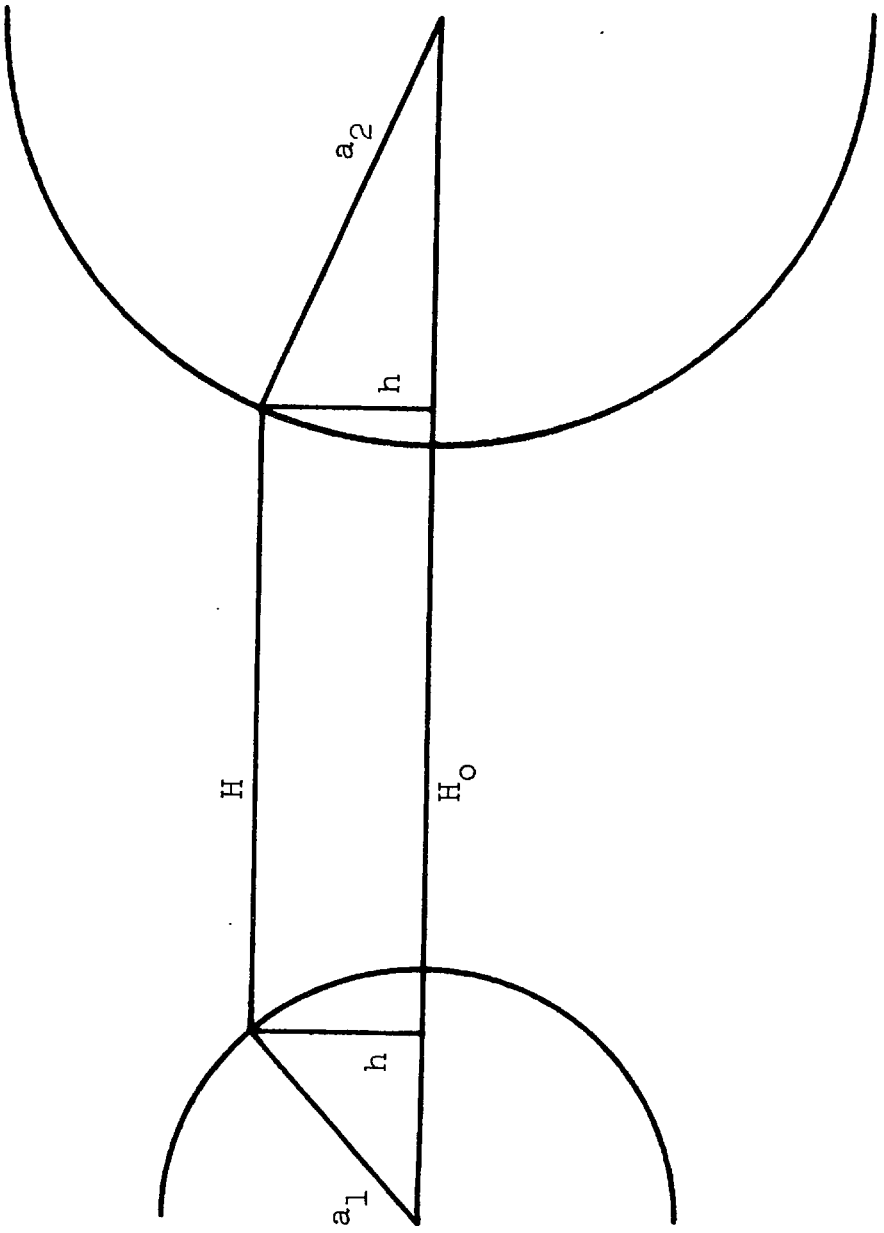

Figure 22. Illustrating the building up of attraction between two unequal spheres via parallel flat plates (70).

and

$$V'_{A(S_1/S_2)} = 2\pi \left(\frac{a_1 a_2}{a_1 + a_2}\right) \int_H^\infty V'_{A(p/p)} dH \qquad \text{(Eq. I-14)}$$

The edge effects are neglected. Finally, the limiting expression for the interaction energy for unequal spheres is

$$V'_{A(S_1/S_2)} = \frac{A a_1 a_2}{(a_1 + a_2)} \left[- \frac{2.45\lambda}{60\pi H^2} + \frac{2.17\lambda^2}{360\pi^2 H^3} - \frac{0.59\lambda^3}{1680\pi^3 H^4} \right] \qquad \text{(Eq. I-15)}$$

$$(\text{for } H \ll a_1,\ a_2;\quad 0.5 < p_o < \infty)$$

Since $p_o = 2\pi H/\lambda$ and λ is usually taken as 10^{-5}cm, equation I-15 should not be used for approximately $H < 150^{o}A$. It is noteworthy that the equation reduces to the identical expression[10] obtained by Schenkel and Kitchener for interaction of equal spheres, i.e. $a_1 = a_2$.

For the range below $p_o = 0.5$, the retardation effect is still significant until the interparticle distance is comparatively very small, in which case equation I-1 will apply. Based on extrapolation of the attractive potential energy curve, an empirical expression that represents the region $0 < p_o < 2$, approximately $H < 300^{o}A$, is

$$V'_{A(S_1/S_2)} = - \frac{A a_1 a_2}{6(a_1 + a_2)H} \left(\frac{\lambda}{\lambda + 11.116H}\right), \qquad \text{(Eq. I-16)}$$

$$(a_1,\ a_2 \gg H)$$

By means of equations I-15 and I-16, the potential energy of attraction between unequal spheres in most colloidal dispersions, emulsions, and suspensions can be calculated.

---

[10] See equation (x) in the appendix of reference 52.

APPENDIX II

Repulsive Potential Energy Between Unequal Spheres

Hogg et. al. (9) derived a general equation for the potential energy of double layer repulsion between unequal spheres.

$$V_{R(S_1/S_2)} = \frac{\varepsilon a_1 a_2 (\psi_{o1}^2 + \psi_{o2}^2)}{4 (a_1 + a_2)} \qquad \text{(Ex. II-1)}$$

$$X \left[\frac{2\psi_{o1}\psi_{o2}}{(\psi_{o1}^2 + \psi_{o2}^2)} \ln\left(\frac{1 + \exp(-KH)}{1 - \exp(-KH)}\right) + \ln(1-\exp(-2KH)) \right]$$

where the assumptions and terms have been defined before. This equation is significant since it applies to two interacting spheres that may have dissimilar surface composition leading to different suface potential values of positive and/or negative signs.

If the surface potential of the unequal spheres are the same, i.e. $\psi_{o1} = \psi_{o2} = \psi_o$, equation II-1 reduces to equation 27. Furthermore, if the spheres are equal in size, i.e. $a_1 = a_2 = a$, the familiar expression of Derjaguin (69, 70) is recognized,

$$V_R = \frac{\varepsilon a \psi_o^2}{2} \ln [1 + \exp(-KH)] \qquad \text{(Eq. II-2)}$$

When the surface constitution are dissimilar and ψ_{o1} and ψ_{o2} are opposite in sign, the value of repulsive potential energy will be negative and mutual attraction results.

APPENDIX III

Interaction Potential Energies Between a Sphere and an Infinitely Large Flat Plate

Retarded Attractive Potential Energy Case

Due to Hamaker (10), the potential energy of attraction between a sphere and an infinitely, long, thick flat plate, $V_{A(S/p)}$, can be described by the following expression:

$$V_{A(S/p)} = -\frac{A}{6}\left[\frac{2a(H+a)}{H(H+2a)} - \ln\left(\frac{H+2a}{H}\right)\right] \quad (a>>H) \qquad \text{(Eq. III-1)}$$

When the sphere and the plate are very close, the limiting expression of equation III-1 is

$$V_{A(S/p)} \sim -\frac{Aa}{12H} \qquad \text{(Eq. III-2)}$$

In a different manner of derivation, Clayfield and Lumb (72) arrived at the same expression as equation III-1. However, on account of the significance of the retardation effect of the London energy between atoms, previously pointed out in Appendix I, the above equations have limited usefulness for extended distances.

In deriving appropriate expressions for the attractive potential energy with the retardation effect, the result of equation I-6 for the potential energy between an atom and a flat plate, $V'_{A(at./p)}$, is used:

$$V'_{A(at./p)} = -\frac{2.45q\lambda\mu}{20}\left(\frac{1}{R^4}\right) + \frac{2.17q\lambda^2\mu}{60\pi}\left(\frac{1}{R^5}\right) - \frac{0.59q\lambda^3\mu}{168\pi^2}\left(\frac{1}{R^6}\right)$$

(Eq. III-3)

Using the approach by Clayfield and Lumb and the geometry in Fig. 23, the retarded interaction energy between a sphere and an infinitely large flat plate, $V'_{A(S/p)}$, can be expressed in integral form by

$$V'_{A(S/p)} = \int_{H}^{H+2a} q\pi y^2 V'_{A(at./p)}\, dR \qquad \text{(Rq. III-4)}$$

where $q\pi y^2 dR$ is the number of atoms in the incremental disc element within the sphere and $y^2 = a^2 - [(H + a) - R]^2$. The solution to equation III-4 is

$$V'_{A(S/p)} = -\frac{2.45A\lambda a^3}{15\pi H^2 (H + 2a)^2} + \frac{2.17A\lambda^2 a^3}{45\pi^2 H^3}\left[\frac{a + H}{(H + 2a)^3}\right] - \frac{0.59A\lambda^3 a^3}{630\pi^3 H^4}\left[\frac{6a^2 + 20a^2H + 5H^2}{(H + 2a)^4}\right] \qquad \text{(Eq. III-5)}$$

$$(\text{for } a >> H;\ 0.5 < p_o = 2\pi H/\lambda < \infty)$$

and its limiting solution is

$$V'_{A(S/p)} \sim Aa\left[-\frac{2.45\lambda}{60\pi H^2} + \frac{2.17\lambda^2}{360\pi^2 H^3} - \frac{0.59\lambda^3}{1680\pi^3 H^4}\right]$$

(Eq. III-6)

Since λ is usually taken as 10^{-5}cm, equations III-5 and III-6 can be used for the approximation of the retarded attractive energy for $H \gtrsim 150^{o}$A. However, equation III-5 is a better approximation than equation III-6 as H approaches a. It is noteworthy that equation III-6 can be derived from the interaction energy between two unequal spheres in the limit where one sphere is much larger than the other (see equation I-15, Appendix I).

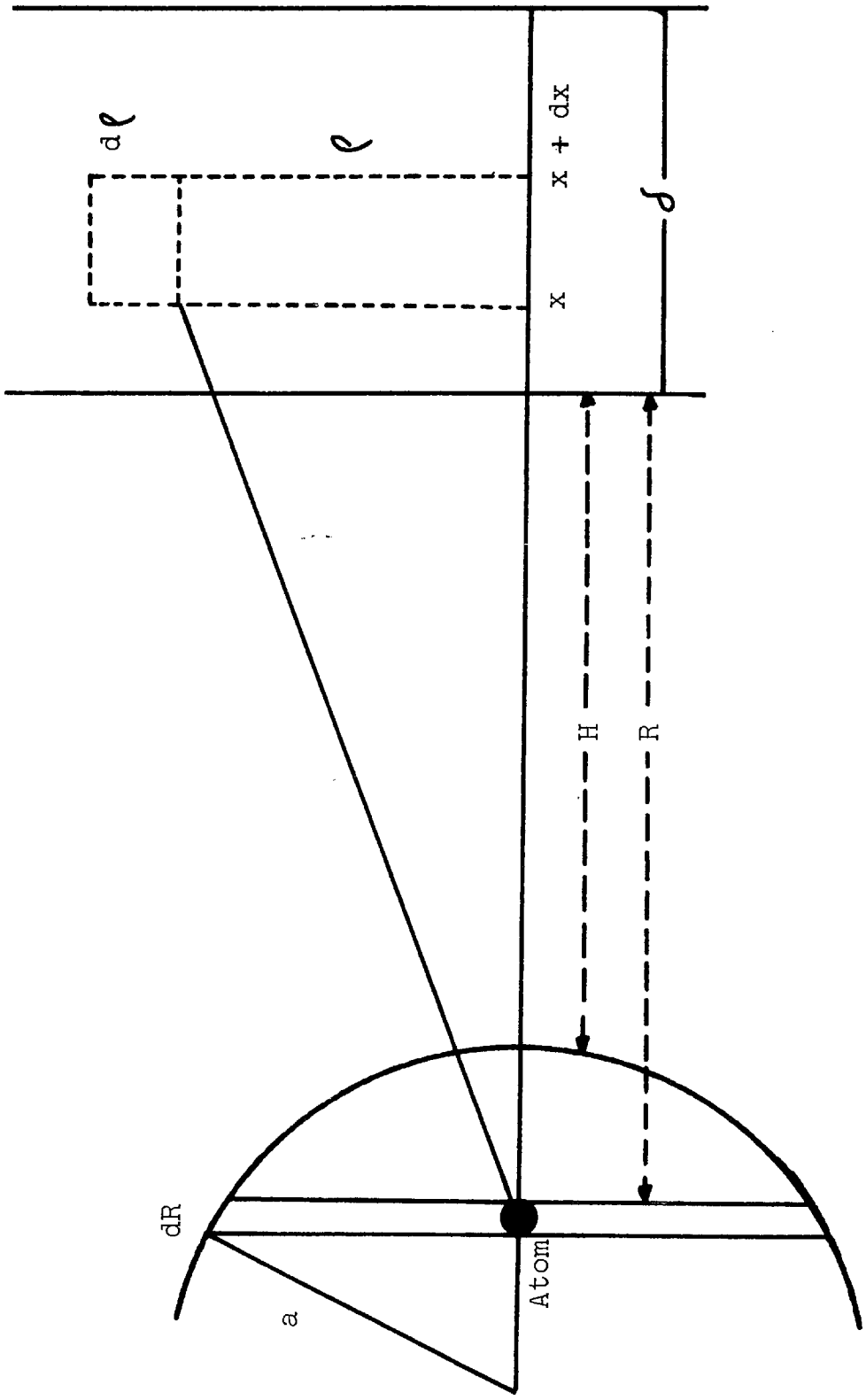

Figure 23. Geometry of the London-Van der Waal interaction between a sphere and an infinitely large flat plate (72).

All that remains is the retarded interaction energy for $H \lesssim 150^{o}A$. This can be approximated by the following equation:

$$V'_{A(S/p)} = - \frac{Aa}{6H} \left(\frac{\lambda}{\lambda + 11.116H}\right) \qquad \text{(Eq. III-7)}$$

Thus, by means of equations III-5 to III-7, the retarded potential energy of attraction between a sphere and a flat plate can be calculated.

Repulsive Potential Energy Case

The general expression for the double layer repulsive potential energy between a sphere and an infinitely large flat plate can be derived in the following way. From Hogg et. al. (9) the interaction energy of two parallel, infinite, flat double layers, $V_{R(p/p)}$, for surfaces of dissimilar constitution is expressed by

$$V_{R(p/p)} = \frac{\varepsilon K}{8\pi} \left[(\psi_{o1}^2 + \psi_{o2}^2) \text{ (1-coth } KH) + 2\psi_{o1}\psi_{o2} \text{ csech } KH\right] \qquad \text{(Eq. III-8)}$$

where the terms have been defined before. Using the Derjaguin approach, in which the surfaces of the sphere and the flat plate is assumed to be built up of parallel pairs of infinitely small rings of radius h (see Fig. 24), the expression for the repulsive energy is

$$V_{R(S/p)} = \int_{o}^{\infty} 2\pi h \, V_{R(p/p)} \, dh \qquad \text{(Eq. III-9)}$$

The edge effects are neglected. From the geometry,

$$H - H_o = a - \sqrt{a^2 + h^2} \qquad \text{(Eq. III-10)}$$

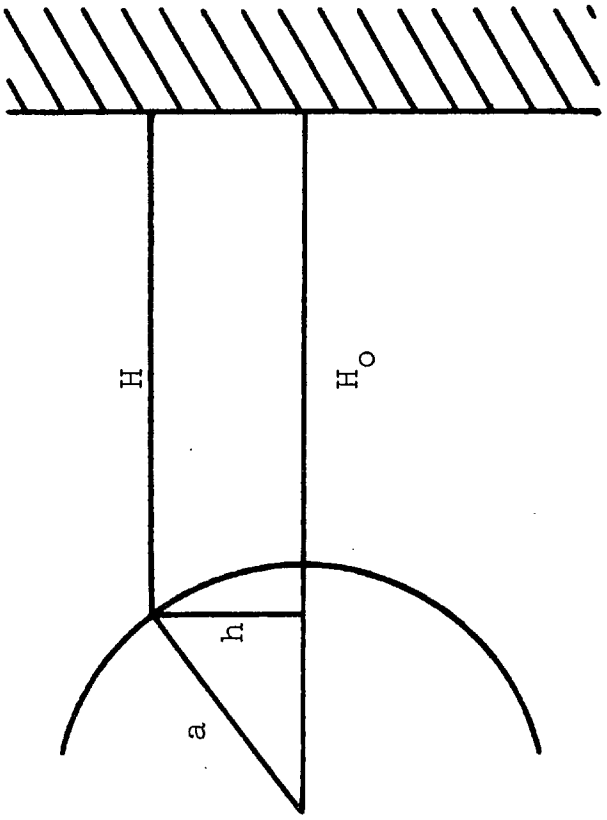

Figure 24. Geometry of interacting quasi-parallel electrical double layers between a sphere and an infinitely large flat plate.

and in the limit that $a \gg h$,

$$adH \simeq hdh \qquad \text{(Eq. III-11)}$$

It follows that the analytic solution of equation III-9 is

$$V_{R(S/p)} = \frac{\varepsilon a}{4} (\psi_{o1}^2 + \psi_{o2}^2) \left[\frac{2\psi_{o1}\psi_{o2}}{(\psi_{o1}^2 + \psi_{o2}^2)} \right.$$

$$\left. X \ln \frac{1 + \exp(-KH)}{1 - \exp(-KH)} + \ln (1-\exp(-2KH)) \right] \qquad \text{(Eq. III-12)}$$

$$(Ka \gg 1)$$

It is observed that the above equation is also the same expression as equation II-1 in the limit that $a_1 \gg a_2$. As in Appendix II, one can analyze the equation for various situations when $\psi_{o1} = \psi_{o2} = \psi_o$ and ψ_{o1} and ψ_{o2} are opposite in sign.

LIST OF REFERENCES

1. Higuchi, W. I., and Misra, J., J. Pharm. Sci., 51 459 (1962).
2. Sherman, P., J. Phys. Chem., 67, 2531 (1963).
3. Wiley, R. M., J. Colloid Sci., 9, 426 (1954).
4. Gillespie, T., J. Phys. Chem., 62, 1303 (1958).
5. Kruyt, H. R., "Colloid Science," Vol. I, Elsevier Publishing Co., Amsterdam, The Netherlands, 1952, p. 278.
6. Van den Tempel, M., Rec. Trav. Chim., 72, 419 (1953).
7. Voyutskii, S. S., Russian Chem. Rev., 30, 556, (1961).
8. Verwey, E. J. W., and Overbeek, J. T. G., "Theory of the Stability of Lyophobic Colloids," Elsevier Publishing Co., Amsterdam, The Netherlands, 1948, p. 176.
9. Hogg, R., Healy, T. W., and Fuerstenau, D. W., Trans. Farad, Soc., 62, 1638 (1966).
10. Hamaker, H. C., Physica, 4, 1058 (1937).
11. Frankel, W., and Reitman, R., "Gradwohl's Clinical Laboratory Methods and Diagnosis," 6th ed., Vol. I, C. V. Mosby, St. Louis, Mo., 1964, p. 109.
12. Cantarow, A., and Trumper, M., "Clinical Biochemistry," 6th ed., W. B. Saunders Co., Philadelphis, Pa., 1962, p. 164.
13. Maclagan, N. F., Brit. Med. J., 2, 892 (1948).
14. Armas-Cruz, R., et. al., Gastroenterology, 35, 298 (1958).
15. Wuhrman, F., and Wunderly, C., "The Human Blood Proteins," 3rd ed., Grune and Stratton, Inc., New York, N. Y., 1960, p. 155.
16. Saifer, A., Am. J. Med., 13, 730 (1952).

17. Wuhrman, F., and Wunderly, C., "The Human Blood Proteins," 3rd ed., Grune and Stratton, Inc., New York, N. Y., 1960, p. 141.

18. Huggins, C., and Jensen, E. V., J. Biol. Chem., 179, 645 (1949).

19. Huggins, C., et. al., Cancer Research, 9, 177 (1949).

20. Huggins, C., "The Scienfific Contributions of the Ben May Laboratory for Cancer Research," The University of Chicago, Chicago, Ill., 1961, p. 105.

21. Frankel, W., and Reitman, R., "Gradwohl's Clinical Laboratory Methods and Diagnosis, 6th ed., Vol. II, C. V. Mosby, St. Louis, Mo., 1964, p. 1148.

22. Ibid., p. 1285.

23. Harris, J. W., "Progress in Hematology," Vol. II, L. M. Tocantins, ed., Grune and Stratton, New York, N. Y., 1959, p. 47.

24. Biozzi, G., et. al., J. Lab. Clin. Med., 51, 230 (1958).

25. Torrance, H., and Glowenlock, A., Clin. Sci., 22, 413 (1962).

26. Taplin, G., Groswold, M., and Dore, E., UCLA Report 481 (Biology and Medicine), 1961.

27. Henkin, R., and Bishop, H., J. Lab. Clin. Med., 60, 709 (1962).

28. Taplin. G. V., et. al., J. Nucl. Med., 5, 264 (1964).

29. Harper, P. V., et. al., "Radioactive Pharmaceuticals," G. A. Andrews, et. al., ed., U. S. Atomic Energy Commission, Oak Ridge, Tenn., 1966, p. 335.

30. Ho, N., Drug Intelligence, 1, 7 (1967).

31. Vessey, I., and Kendall, C. E., Analyst, 91, 273 (1966).

32. Garvan, J. M., and Gunner, B. W., Med. J. Australia, 2, 140 (1963).

33. Ibid., 2, 1 (1964).

34. Lockhardt, J. D., "Proceedings of the F. D. A. Symposuim on Safety of Large Volume Parenteral Solutions," Washington, D. C., July 28-29, 1966.

35. Gross, M. A., Drug Intelligence, 1, 12 (1967).

36. Anon, ibid., 1, 21 (1967).

37. Hardaway III, R. M., "Syndrome of Disseminated Intravascular Coagulation," Charles C. Thomas, Springfield, Ill., 1966, ch. 6 and 9.

38. Groves, M. J., and Major, J. F., Pharm. J., 193, 227 (1964).

39. Groves, M. J., J. Pharm. Pharmacol., 18, 161 (1966).

40. Kruyt, H. R., "Colloid Chemistry," Vol. I, Elsevier Publishing Co., Amsterdam, The Netherlands, 1952, p. 286.

41. Martynov, G. A., and Bakanov, S. P., "Research in Surface Forces," B. Derjaguin, ed., Trans. by the Consultants Bureau, New York, N. Y., 1963.

42. Swift, D. L., and Friedlander, S. K., J. Colloid Sci., 19, 621 (1964).

43. Rice, C. L., and Whitehead, R., J. Colloid Sci., 23, 174 (1967).

44. Hidy, G. M., ibid, 20, 123 (1965).

45. Hidy, G. M., and Lilly, D. K., ibid., 20, 341, 867 (1965).

46. Gillespie, T., ibid., 18, 562 (1963).

47. Kruyt, H. R., "Colloid Chemistry," Vol. I, Elsevier Publishing Co., Amsterdam, The Netherlands, 1952, p. 283.

48. Fuchs, N., Z. Physik, 89, 736 (1934).

49. Reerink, H. and Overbeek, J. T. G., Disc. Farad. Soc., 18, 74 (1954).

50. Srivastava, S. N., and Haydon, D. A., Trans. Farad. Soc., 60, 971 (1964).

51. Srivastava, S. N., Indian J. Chem., 3, 376 (1965).

52. Schenkel, J. H., and Kitchener, J. A., Trans. Farad. Soc., 56, 161 (1960).

53. Simpson, R. B., and Kauzmann, W., J. Am. Chem. Soc., 75, 5139 (1953).

54. Stark, G., Stein, W., and Moore, S., J. Biol. Chem., 235, 3177 (1960).

55. Kubitschek, H. E., Research (London), 13, 128 (1960).

56. Samyn, J., J. Pharm. Sci., 54, 1794 (1965).

57. Frensdorff, H., Watson, M., and Kauzmann, W., J. Am. Chem. Soc., 75, 5157 (1953).

58. Steven, F. and Tristam, G., Biochem. J., 73, 86 (1959).

59. Gagen, W. and Home, J., J. Phys. Chem., 68, 723 (1964).

60. Tanford, C., "Physical Chemistry of Macromolecules," John Wiley and Sons, Inc., New York, N. Y., 1961, p. 627.

61. Joly, M., "A Physico-Chemical Approach to the Denaturation of Proteins," Academic Press, New York, N. Y., 1965, p. 28 and 38.

62. Kruyt, H. R., "Colloid Chemistry," Vol. I, Elsevier Publishing Co., Amsterdam, The Netherlands, 1952, p. 291.

63. Ho, N., "Current Methodology of Determining Size and Number of Particles in Parenteral Solutions," Presented to the Food and Drug Administration, Washington, D.C., May 18, 1967.

64. Lachman, L., "Proceedings of the F. D. A. Symposuim on Safety of Large Volume Parenteral Solutions, Washington, D.C., July 28-29, 1966.

65. Vold, M., J. Colloid Sci., 16, 1 (1961).

66. Fowkes, F. M., "Chemistry and Physics of Interfaces," D. Gushee, ed., American Chemical Society Publications, Washington, D.C., 1965, p. 1.

67. Kruyt, H. R., "Colloid Science," Vol. I, Elsevier Publishing Co., Amsterdam, The Netherlands, 1952, p. 266.

68. Casimir, H. B., and Polder, D., Phys. Rev., 73, 360 (1948).

69. Derjaguin, B., Kolloid Z., 69, 155 (1934).

70. Verwey, E. J. W., and Overbeek, J. T. G., "Theory of the Stability of Lyophobic Colloids," Elsevier Publishing Co., Amsterdam, The Netherlands, 1948, p. 137.

71. Ibid., p. 102.

72. Clayfield, E. J., and Lumb, E. C., J. Colloid Sci., 22, 269 (1966).